Virginia Commonwealth University

VCU Scholars Compass

2010

Development of Electroencephalography based Brain Controlled Switch and Nerve Conduction Study Simulator Software

Kai Qian
Virginia Commonwealth University

School of Engineering
Virginia Commonwealth University

This is to certify that the thesis prepared by Kai Qian entitled "Development of Electroencephalography based Brain Controlled Switch and Nerve Conduction Study Simulator Software" has been approved by his committee as satisfactory completion of the thesis requirement for the degree of Master of Science.

Ou Bai, Ph.D., Director of Thesis, School of Engineering

Ding-Yu Fei, Ph.D., School of Engineering

Scott Vota, D.O., Department of Neurology, VCU Medical Centre

Gerald Miller, Ph.D., Chair, Department of Biomedical Engineering, School of Engineering

Rosalyn Hobson, Ph.D., Associate Dean of Graduate Studies, School of Engineering

Russell Jamison, Ph.D., Dean, School of Engineering

F. Douglas Boudinot, Ph.D., Dean of the Graduate School

Date

DEVELOPMENT OF AN ELECTROENCEPHALOGRAPHY-BASED BRAIN

CONTROLLED SWITCH AND NERVE CONDUCTION STUDY SIMULATOR

SOFTWARE

A thesis submitted in partial fulfillment of the requirements for the degree of Master of Science at Virginia Commonwealth University.

by

KAI QIAN
B.S., East China University of Science and Technology, People's Republic of China, 2005

Director: OU BAI, PH.D.
Assistant Professor, Department of Biomedical Engineering

Virginia Commonwealth University
Richmond, Virginia
December, 2010

Acknowledgments

I would like to express my gratitude to my adviser Dr. Ou Bai for your continuous support of my study and research. Thank you for your guidance and encouragement that make this thesis possible. I also would like to thank my thesis committee members: Dr. Ding-Yu Fei and Dr. Scott Vota. Thank you for your insightful comments and help in completion of my thesis project. My sincere thanks also goes to Dr. Chike Linton who helped me gather the data and gave me numerous advices on improvements of my research project.

I would also like to thank Ms. Cai-Ting Fu and my lab mates Dandan Huang, Deepak Kumbhare, Vaishnavi Karnad, Mason Montgomery, Plamen Nikolov, and William Eggleston for your help in my experiment and study.

Lastly, and most importantly, I wish to thank my parents, Enxia Shi and Fenguan Qian. They gave me life, raised me, support me, teach me and love me. To them I dedicate this thesis.

Table of Contents

iv

List of Abbreviations

ALS	Amyotrophic Lateral Sclerosis
ANOVA	One-way Analysis of Variance
BCI	Brain-Computer Interface
CNS	Central Nervous System
DTC	Decision Tree Classifier
ECoG	Electrocorticography
EEG	Electroencephalography
EMG	Electromyography
EOG	Electrooculogram
ERD	Event-Related Desynchronization
ERS	Event-Related Synchronization
FFT	Fast Fourier Transform
GA	Genetic Algorithm
GA-MLD	Genetic Algorithm Based Mahalanobis Linear Distance
GUI	Graphical User Interface
LFP	Local Field Potentials
MLD	Mahalanobis Linear Discriminator
PSD	Power Spectrum Density
SLD	Surface Laplacian Derivation

NCS	Nerve Conduction Study
LAC	Lateral Antebrachial Cutaneous
MAC	Medial Antebrachial Cutaneous

List of Tables

List of Figures

Abstract

DEVELOPMENT OF AN ELECTROENCEPHALOGRAPHY-BASED BRAIN

CONTROLLED SWITCH AND NERVE CONDUCTION STUDY SIMULATOR

SOFTWARE

By Kai Qian, M. S.

A thesis submitted in partial fulfillment of the requirements for the degree of Master of Science at Virginia Commonwealth University.

Virginia Commonwealth University, 2010

Major Director: Ou Bai, Ph.D.
Assistant Professor, Department of Biomedical Engineering

This thesis investigated the development of an EEG-based brain controlled switch and the design of a software for nerve conduction study.

For EEG-based brain controlled switch, we proposed a novel paradigm for an online brain-controlled switch based on Event-Related Synchronizations (ERDs) following external sync signals. Furthermore, the ERD feature was enhanced by 3 event-related moving averages and the performance was tested online. Subjects were instructed

x

to perform an intended motor task following an external sync signal in order to turn on a virtual switch. Meanwhile, the beta-band (16-20Hz) relative ERD power (ERD in reverse value order) of a single EEG Laplacian channel from primary motor area was calculated and filtered by 3 event-related moving average in real-time. The computer continuously monitored the filtered relative ERD power level until it exceeded a pre-set threshold selected based on the observations of ERD power range to turn on the virtual switch. Four right handed healthy volunteers participated in this study. The false positive rates encountered among the four subjects during the operation of the virtual switch were $0.8 \pm 0.4\%$, whereby the response time delay was 36.9 ± 13.0s and the subjects required approximately 12.3 ± 4.4 s of active urging time to perform repeated attempts in order to turn on the switch in the online experiments.

The aim of nerve conduction simulator software design is to create software that can be used by nerve conduction simulator to serve as a medical simulator or education tool to train novice physicians for nerve conduction study test. The real response waveform of 10 different upper limb nerves in conduction studies were obtained from the equipment used in real patient studies. A waveform generation model was built to generalize the response waveform near the standard stimulus site within study interest region based on the extracted waveforms and normal reference parameters of each study and stimulus site coordinates. Finally, based on the model, a software interface was created to simulate 10 different nerve conduction studies of the upper limb with 9 pathological conditions.

xi

Part 1 Development of Electroencephalography based Brain Controlled Switch

CHAPTER 1

Introduction

1.1 Background

Brain-computer interfaces (BCIs) provide an augmented communication channel for individuals who do not have the motor function capabilities necessary to interact with the external world by controlling a device, such as robotic arm, wheel chair, or computer (Wolpaw et al. 2002), and also for able bodied individuals to interact with media applications such as Google earth (Scherer et al. 2007), virtual environment (Scherer et al. 2008) as a new human machine interface, or even prove suitable as a biometric measure for person identification (Pfurtscheller & Neuper 2006; Pfurtscheller & Solis-Escalante 2009).

Generally, BCI system consists of four parts, i.e., signal recording, signal processing, prediction, and external device control. In signal recording part, electrodes are used to record brain derived signals. The recorded signals are amplified and before sending to the signal processing part. Through spacial and temporal filtering in signal processing part, signal features in terms of amplitude or frequency power are extracted. Prediction part determines cognitive or motor intention that is reflected from brain

activity changes based on the signal features. Finally, external device control part converts prediction results to commands that drive different external devices.

BCI systems can be divided into two types, noninvasive and invasive, by signal recording site.

Noninvasive BCI, one of which that is most often used is known as electroencephalography (EEG)-based BCI, uses EEG signals recorded from the scalp to drive BCI system. Most studies in humans have been using EEG, since the recording method is inexpensive, convenient and has low risk. However, signal quality of EEG is poor. It represents ensemble electrophysiological activity of a large number of neurons over cortex. The EEG rhythms do not contain specific information about the details of movements such as position or velocity information of limb movement. Another factor that leads to the low quality of EEG signal is the volume conduction which makes the EEG signals very vulnerable to artifacts such as eye blinks and muscle movement. Despite of these short comings, by far the majority of the clinical applications of BCI technologies in people with severe motor disabilities have been demonstrated using EEG (Kubler et al. 2005; Nijboer et al. 2008). The EEG-based BCI applications include cursor control, wheelchair control, switch control and so on.

Invasive BCI utilizes signals recorded inside the brain. Single unit recording has the micro-electrode arrays implanted in the brain parenchyma to acquire single neuron activity. The recorded spikes train and local field potential provide rich information on human motor function for BCI to translate it into command to control the kinematics of robot arm(Georgopoulos, Schwartz & Kettner 1986; Wang et al. 2007). Another invasive BCI system is Electrocorticography (ECoG)-Based BCI which records signal from

2

cortical surface directly. ECoG signal allows BCI system to use information from higher frequency band, gamma band, which EEG could not provide due to its poor signal quality. Although quality increases as recording goes deeper inside the brain, two major barriers still remain. One is that the brain tissue damage by electrodes implant may cause CNS infection. The other is that the encapsulation of electrodes by immune response inside body will decrease electrodes electrical conductivity making it hard for long term use (Seymour & Kipke 2007).

BCI systems can also be divided into synchronize and asynchronous system by operation mode.

Synchronous BCI

Users of synchronous BCI have to synchronize with the system cues to perform cognitive or motor tasks that induced the brain activity changes in order to drive BCI system (Wolpaw & McFarland 1994; Birch & Mason 2000). It is also known as cue-based BCI system. The majority of current BCIs research falls into this category.

Asynchronous BCI

In contrast to synchronous BCI, users decide when to perform the cognitive or motor tasks to drive BCI system, and the system has to figure out when the task happens. It is also known as self-paced BCI system. It is more natural for user control but much harder for system realization(van Gerven et al. 2009).

3

1.2 Objective

Most of EEG-BCI investigations have been performed to achieve trial-based continuous controls. An example of the aforementioned control includes the cursor control introduced by Wolpaw's group, wherein a cursor at left side of monitor starts moving at the beginning of each trial while requiring the users to keep sustained attention and continuously regulate their brain activities to control cursor vertical position until the cursor reaches the right side of the monitor (Wolpaw et al. 1991; McFarland, Sarnacki & Wolpaw 2003). In contrast to the trial-based BCI designs, a couple of research groups explored self-paced or asynchronous designs for continuous BCI operation to differentiate 'Intentional Control' state from 'No Control' state; Birch's group employed a slow cortical potentials (SCP)-like low frequency EEG signals, formally known as low-frequency asynchronous switch design (LF-ASD) (Mason & Birch 2000; Birch, Bozorgzadeh & Mason 2002) or the improved versions (Bashashati et al. 2006), Pfurtscheller's group employed Mu rhythm-based event-related desynchronization (ERD) design (Pfurtscheller et al. 2005; Muller-Putz et al. 2006), as well as a SSVEP-based self-paced BCI approach (Parini et al. 2009). The majority of literatures related to the self-paced or asynchronous BCI were performed offline to explore optimal computational methods (Faradji, Ward & Birch 2009; Scherer, Muller-Putz & Pfurtscheller 2009; Fatourechi, Ward & Birch 2008b), whereas online study is still limited.

We consider the following properties in developing a brain-controlled switch as functional as a real-world switch:

Self-paced: for a real-world switch, for example, a light switch, users will pay attention to the switch only when they want to turn the switch on/off. Birch's group addressed that

4

the users may perform a certain motor task only when they want the 'Intentional control' of the BCI system, whereas users may be day-dreaming, thinking about a problem or any other tasks other than the motor task for the 'Intentional Control' during the 'No Control' State (not to operate the switch) (Bashashati et al. 2006). Ideally, a fully self-paced brain-controlled switch will allow users to do any tasks other than the task for 'Intentional Control' or just keep relax when they don't intend to operate the switch. However, due to the low signal-to-noise (S/N) ratio of the brain signals when recorded noninvasively from EEG, current self-paced BCIs are not completely free from mental tasks and the users are still attentive during 'No Control' State (Birch, Bozorgzadeh & Mason 2002). For example, subjects were asked to count the number of times that a white ball bounced off the monitor's screen during 'No Control' state (Fatourechi, Ward & Birch 2008b). It is more plausible to develop a self-paced brain-controlled switch that may allow users not to attend to a particular task or tasks. Moreover, for BCI applications, users may achieve other control purposes with certain mental tasks if they don't need to keep attentive to the switch.

Minimal false positive rate (FPR): considering that a real-world switch mostly stays in off-activation state, the brain-controlled switch should have minimal FPR to avoid false triggering during the 'No Control' State. For example, a FPR of 10% may result in about 15 incorrect operations or erroneous operations in just 10 minutes, assuming that the brain-controlled switch detects the brain signal every 4 s. Birch's group suggested that 0% FPR might be required in practical applications and achieved averaged FPR below 1% in their offline or pseudo-online optimization studies (Faradji, Ward & Birch 2009; Fatourechi, Ward & Birch 2008a).

Interactive: the operation of a real-world switch is interactive that allows users to make multiple attempts until the switch is activated, because not all the switches are necessary to be sensitive enough that can be activated in a single attempt. It is particularly important for a brain-controlled switch that the interactive operation is required to achieve low FPR under a higher activation threshold. The current self-paced or asynchronous BCI adopted TPR to evaluate the sensitivity of BCI in the 'Intentional Control' state. For a real world switch, users need not to keep operating the switch after the switch is activated. Therefore, a response time showing how fast the switch is activated will be more appropriate to provide the switch performance.

Mental operation: the BCI was originally proposed to restore motor functions for paralyzed patients, who may be unable to make muscle contraction to produce physical movement. Pfurtscheller's group explored motor imagery-based asynchronous BCI to allow paralyzed patients to 'walking' in a virtual environment (Leeb et al. 2007). In the early Brich's group study, they also investigated the feasibility of a motor imagery-based self-paced BCI (Birch, Bozorgzadeh & Mason 2002).

The event-related frequency power decrease, or event-related desynchronization (ERD) has patterns in certain frequency bands and specific sites characterizing the dynamics of EEG oscillation time-locked to an externally triggered event, which are highly reproducible and stable over time (Pollock, Schneider & Lyness 1991; Kondacs & Szabo 1999; Pfurtscheller et al. 2006). The ERD patterns can also be observed when subjects perform voluntary movement or intended motor imagery tasks over motor areas contralateral to the hand moved or imagined (Pfurtscheller & Lopes da Silva 1999). These merits promote the ERD feature as a better choice to drive BCIs.

6

In this study, we proposed a novel paradigm for a brain-controlled switch based on human motor imagery-associated ERD following external sync signals. In this paradigm, the ERD feature was enhanced by consecutive event-related moving average time-locked to the external sync signal. Assuming that the smoothed EEG power of consecutive epochs provides a better S/N ratio that may tolerate the variances of EEG spontaneous activity, we expected that the novel design of a BCI switch may provide more reliable and robust performance with a minimal false positive rate along with shorter time to turn the switch on. The interactive brain-controlled switch was designed similar to a real-world switch which users would not need to keep sustained attention on the switch (for sample, continuously regulating their brain activities or perform some mental tasks different from the task to turn on the switch), when they did not want to operate the switch. Furthermore, the brain-controlled switch was interactive in the sense that users performed repeated attempts until the switch was turned on. The novel brain-controlled switch was tested online in real-time.

7

CHAPTER 2

Methods

2.1 Subjects

Four right handed healthy volunteers (two females and two males) between the ages of 18 and 26 participated in this study. All subjects gave informed consent. Prior to this study, subjects didn't receive any training related to the regulation of their brain rhythm or were informed of the experimental hypothesis. The protocol was approved by the Institutional Review Board.

2.2 Experimental paradigm and behavioral task

All the subjects participated in 6 sessions of experiments: 1 session with physical movement of right index finger pinch and 5 sessions with motor imagery of finger movement. The first session with physical movement was for comparison purpose only. Subjects were asked to successfully turn on a virtual switch provided on a computer monitor 10 times in each session. Additionally, a short calibration session was performed at the beginning of the experiment, and each experiment lasted approximately 3-4 hours.

During the recording, subjects were seated in a chair with the forearms semi-flexed and supported by a pillow. They were asked to keep all muscles relaxed, except

8

for those in the right hand; also, each subject was instructed to avoid any excessive eye movements, blinks, body adjustments, swallowing or other body movements during the visual cue onset. During motor imagery, the investigator monitored the EMG activity continuously, and once EMG activity was observed subjects were reminded to relax the muscles. Epochs with EMG contamination were excluded from offline neurophysiological analysis.

In contrast to the conventional BCI design in which subjects were requested to perform sustained mental/physical tasks to achieve asynchronous control, we developed a novel brain-controlled switch paradigm by introducing an event-related design. Considering that subjects might be easily fatigued from the sustained active mental task, the subjects were able to alternate between a short active task and relaxation in the event-related design so that the required period of sustained attention could be greatly reduced. From our preliminary tests, we found that subjects were comfortable with 1 s active urging the movement following by 2 s relaxations.
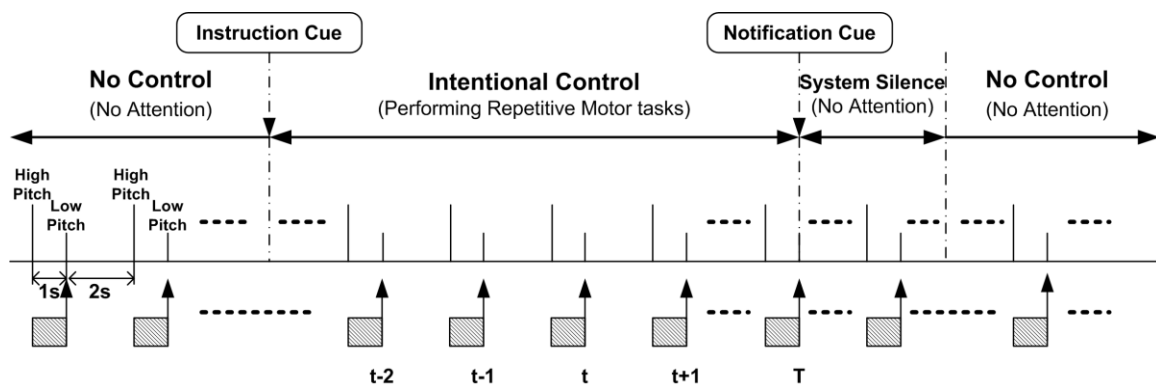

Fig. 1. Experimental paradigm. When subjects perceived a visual instruction that was provided on the computer monitor placed about 1.5 m in front of the subjects (start of 'Intentional Control'), they started to perform the motor tasks of either motor imagery or

9

physical movement of their right index finger pinch following the auditory cues of high and low pitches; they started to urge their motor tasks by motor imagery/physical movement as soon as they heard a high pitch sound and after hearing a low picth sound ,then relaxed; they repeated the motor tasks until the virtual switch was turned on thus marking the end of the 'Intention Control' and start of the 'System Silence', which kept about 20 s. During the 'System Silence' and 'No Control'state, subjects remained relaxed and were free from the any particular tasks until the start of the next task state. The duration of the 'No Control' state was a random period between 20 and 30 s. During both the 'Intentional Control', 'System Silence' and 'No Control' state, the computer calculated the frequency power at every low pitch sound. The frequency power was estimated from the continuously extracted signals in the time windows between high and low pitches (shaded boxes), when subjects performed motor imagery of active urging for 'Intentional Control'.

The designed experimental paradigm is illustrated in Fig. 1. When the experiment began, subjects were provided a sequence of alternative auditory signals: a high pitch sound ('Di', 5k Hz) and a low pitch sound ('Da', 2k Hz). The auditory sound of 'Di' and 'Da' alternated throughout the experiment to serve as an external sync signal. Both the durations of the high low pitch sounds were 200 ms. The interval between the high pitch sound and low pitch sound was 1 s, and the interval between the low pitch sound and the next high pitch sound was 2 s. The entire time period of 3 s, i.e. the start of one high pitch sound to the next high pitch sound, constituted one trial. The data for the estimation of frequency power was acquired from the interval between high pitch sound and low pitch sound, where the data length was 1 s. At the beginning of the experiment, subjects were provided a blank screen together with a green bar on its right. A pre-set threshold was

10

provided by a yellow bar; when the green bar exceeded the yellow bar, the virtual switch was turned on.

Each experimental session began from 'No Control' state, where subjects were instructed to avoid either physical or imagined hand movement. No particular tasks were asked to perform and the subjects didn't keep attentive to the switch during 'No Control' state. When a visual instruction cue 'Begin to turn on switch' was provided on the screen, subjects was asked to turn on the virtual switch by performing the instructed motor tasks. This was the beginning of the 'Intentional Control'. A notification cue was provided on the monitor showing that the switch was activated by a positive detection. During the physical movement session, subjects were asked to start urging or intending the motor task when once they heard the high pitch sound, and then promptly to pinch their right thumb and index finger when they heard the following low pitch sound. During the motor imagery sessions, subjects were also asked to urge or intend the motor task when they heard the high pitch sound. They imagined brisk finger pinch movement and subsequently relaxed when they heard the low pitch sound. The active urging to move following by either motor imagery or physical movement was repeated until the switch was turned on. The green bar on the screen went up or down with the estimated frequency power value, which was updated when the low pitch sound was delivered. Once the green bar was higher than the pre-set yellow bar, the virtual switch was turned on and a text message of 'Switch turned on' (Notification cue) was prompted on the screen. This was the end of the 'Intentional Control' state and the start of the 'System Silence' state. During the 'System Silence' and the 'No Control' states, subjects didn't pay attention to the task, relaxed and ignored the sound cues. The text message of

11

'Switch turned on' stayed on the screen for about 20 s during 'System Silence' and was removed to indicate the start of 'No Control' state. During 'System Silence' period, the system didn't make detection to allow the frequency power back to the baseline, because of the event-related moving average. The subjects were not attentive to any particular tasks until the next instruction cue was provided asking to turn on switch.

In the short calibration session at the beginning of the experiment, the subject was kept relaxed while the computer continually calculated the frequency power values which were used for determining the threshold of the online detection.

2.3 Data acquisition and online data processing

EEG was recorded from 9 (tin) surface electrodes (F3,Fz, F4, C3, Cz, C4, P3, Pz, P4), attached on an elastic cap (Electro-Cap International, Inc., Eaton, OH, U.S.A.) according to the international 10-20 system (Jasper & Andrews 1938), with reference from the right ear lobe and ground from the forehead. For surface electromyography (EMG), which was used to monitor the movement, electrodes filled with conductive gel were taped to the right forearm to record extensor digitorum communis (EDC). Electrodes for bipolar electrooculogram (EOG) above left eye and below right eye were also pasted. Signals from all the channels were amplified (g.tec GmgH, Schiedlberg, Austria), filtered (0.1-100 Hz) and digitized (sampling frequency was 256 Hz).

The digitalized signal was then sent to a HP PC workstation and was online processed using a home-made MATLAB (MathWorks, Natick, MA) Toolbox: brain-computer interface to virtual reality or BCI2VR (Bai et al. 2007). The BCI2VR programs served for both the visual stimulus and online processing of the EEG signal.

12

2.4 Computational algorithm

At the time every low pitch sound delivered, the computer concatenated a number of the previous epochs of EEG data between high pitch and low pitch sound from the data acquisition system. The data was spatial filtered by Laplacian reference algorithm (Hjorth 1975) , i.e., reference to surrounding orthogonal channels, for example, channel C3 was referenced to the average of channels P3, Cz, F3. Assuming that ERD is maximized over motor area contralateral to hand moved the referenced channel C3 was selected to control the switch. The power spectral density value was estimated from the spatially filtered signal from channel C3, using Welch Method with FFT length of 64, segment length of 32, overlapping rate of 0.5, where a Hamming window was also employed. Finally the smoothed power spectral density value from frequency bin 5, which corresponded to frequency band (17-20 Hz), was linearly converted to a relative power value of ERD_R, which was calculated by

$$ERD_R = \frac{P_{ref} - P}{P_{ref}} \qquad (1)$$

where P is the power spectral density of ongoing EEG signal, and P_{ref} is a power reference value. The P_{ref} can be determined by the power spectral density value in the idle state. We set P_{ref} a subject-independent value which was the maximum EEG power value of previous EEG experiment. When EEG frequency power associated with human motor intention or urge to move decreases, the value of the relative ERD_R increases. The ERD_R valued was then compared with a pre-set threshold value to determine whether the user intended to turn on the switch or not.

13

When the online calculated ERD_R was lower than the threshold the switch kept off. On the other hand, when the ERD_R was higher than the threshold the switch was tuned on. The threshold was adjusted to fit each subject by manual adjustment during the short calibration session before the 6 sessions of experiments. According to low false positive criterion (described in next section), the threshold value was set to a little larger than the maximum power value of the 'No Control' state during the calibration session.

2.5 Determine the numbers of moving average epochs

Though ERD is a stable physiological phenomenon associated with human voluntary motor control, the ERD may be affected by various neuronal processes that naturally result in a large variance of ERD. The large variance of ERD, therefore, may make the single-trial decoding unreliable. In order to suppress the noise, we proposed an event-related moving average for ERD following the proposed event-related paradigm design. As shown in Fig. 1, the frequency power was calculated continuously following the low pitch sound at time t-2, t,-1, t, t+1, … The data in each time-window between the high pitch sound and low pitch sound, in which subjects were actively urging to move when they were instructed to turn on the switch, was extracted for the power spectral density estimation. For example, to obtain a smoothed power from 3 consecutive epochs, the frequency power at time instant t (see Fig. 1) was calculated by a moving average from 3 epochs/time-window of t-2, t-1 and t. From the statistical point-of-view, a more smoothed ERD feature can be obtained from a larger number of consecutive epochs of data for estimation. However, the more epochs for smoothing, the more time delay required to turn on the switch. To determine a suitable number of the epochs to obtain the moving average for power estimation, we performed a pilot experiment The mean and

14

standard derivation of the ERD_R during 'Intentional Control' state and 'No Control' state were calculated offline.

2.6 Performance evaluation

The performance of the brain-controlled switch was evaluated by 2 indices: the false positive rate (FPR) and the active urging time/response time. FPR was defined as follows,

$$FPR = \frac{FP}{TN + FP} \qquad (2)$$

where FP was the number of false positive detections, i.e., the number of positive detections made during the 'No Control' state, and TN was the number of true negative detections, i.e., the number of true negative detections made during the 'No Control' state. Detection was made following every low pitch delivered (every 3 s).

Because we adopted an event-related design in which the subjects urged to move for 1 s out of every 3 s when they were asked to turn on the virtual switch, the active urging time was the total time that subjects were urging the movement to turn on the switch. The active urging time was proportional to the total number of repeated attempts with one attempt duration of 1 s. The active urging time was also proportional to the response time, i.e. the total time from the starting of the 'Intentional Control' state until the virtual switch was turned on or the start of 'System Silence'.

15

CHAPTER 3

Results

3.1 Time- frequency analysis

The time-frequency analysis during the 'Intentional Control' state and the 'No Control' state is illustrated in Fig. 2. The first column plots were obtained from one session with motor imagery, where subjects were urging to move after they heard a high pitch sound (time 0) and imagined the finger movement after they heard a low pitch sound (time 1). Similarly, the third column plots were obtained from the session with physical movement where subjects were urging to move, but they performed physical movement instead of motor imagery. The second and the fourth column plots were obtained from the data where subjects were relaxed without attentive to any particular tasks. The frequency power in all time-frequency plots was baseline corrected with respect to the power from -0.5 to 0. When subjects were actively urging the movement in the 'Intentional Control' state, the ERD in blue color from a Laplacian referenced C3 channel was observed for both sessions of motor imagery and physical movement. The frequency bands of ERD were in the beta band around 15-30 Hz. The ERD associated with active urging from time 0 to 1 was observed in the session with motor imagery, although the ERD amplitude was smaller for the session with motor imagery than the

16

session with physical movement. The ERD duration in the session with motor imagery was also shorter than the ERD in the session with physical movement. In the 'No Control' state, no ERD was found in the inspected time-window from time 0 to 1. Therefore, the ERD in the beta band provided a potential feature to make true positive detection following 'Intentional Control' and reject false positive detections in the 'No Control' state for both sessions with motor imagery and physical movement. We also noticed that the ERD variance among subjects in the session with motor imagery was large; S1 had a stronger and longer ERD where S4 had a barely recognizable ERD in the active urge window, though the ERD of S4 in the session with physical movement was as large as the ERD of S1.
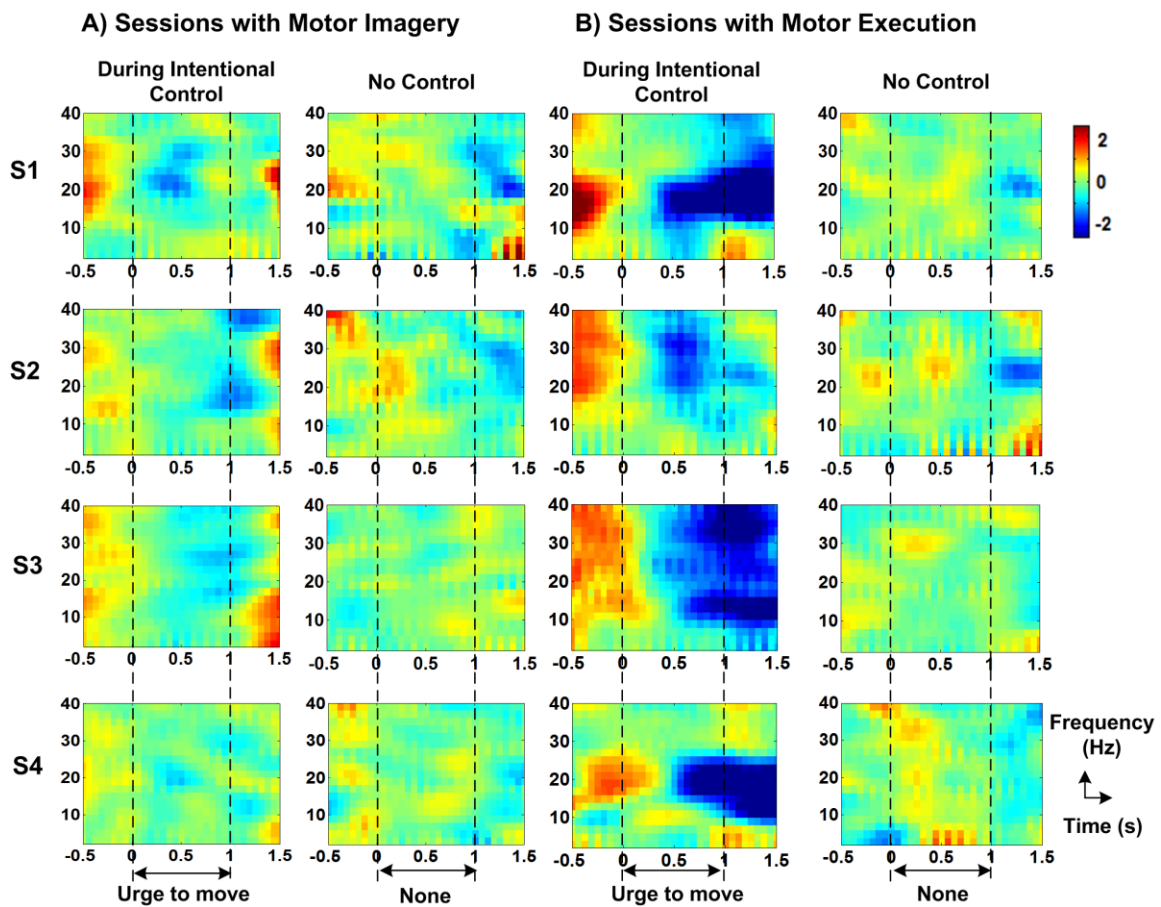
Fig. 2 Time-frequency plots for four subjects from Laplacian referenced C3 channel. The blue color shows frequency power decrease or ERD. Time 0 was the arriving time of the first high pitch sound. Time 1 was the arriving time of the consequent low pitch sound. In the task state that subjects were asked to turn on the virtual switch by motor imagery of active urging during the time period from 0 to 1 s and relax at time 1, or by urging to move during the time period from 0 to 1 s, and to perform the physical movement at time 1. The frequency power decrease or ERD was clearly recognizable in the frequency band 15-20 Hz during the time period that subjects were urging to move. In contrast to the task state, subjects didn't perform any particular tasks during the entire the 'No Control' state. There was no recognizable ERD pattern from time 0 to 1. Compared with the ERD in session with physical movement, ERD associated with urging followed by motor imagery of finger movement was smaller. The variance in the timing and the amplitude of ERD among subjects was also large in the session with motor imagery.

3.2 Determine the numbers of epochs for event-related moving average

The mean and standard deviation of the smoothed ERD_R samples estimated from increasing number of epochs for smoothing as shown in Fig. 3 was obtained from subject 1. There were 54 non-smoothed ERD_R samples for the 'Intentional Control' state and 61 non-smoothed ERD_R samples for the 'No Control' state. As illustrated in Fig. 3, there were significant differences between the mean power values of the 'Intentional Control' state and 'No Control' state for all the numbers of smoothing (1 to 5). This thus confirmed the feasibility of the designed method to potentially differentiate the two aforementioned states.

18

As shown in Fig. 3, when the number of epochs for smoothing was increased, the standard deviation of smoothed ERD_R samples was decreased. These results were consistent with the assumption for brain-controlled switch design that the frequency power of ERD_R smoothed from consecutive epochs following the external sync signal might provide an enhanced feature for differentiating the 'Intentional Control' state and 'No Control' state because of the reduced sample variance/standard deviation in natural EEG rhythmic activity. The standard deviation was decreased more sharply from 1 to 3 epochs' smoothing compared with 3 to 5 epochs' smoothing. More epochs' smoothing provided smaller sample variance so that the differential accuracy of ERD_R would be higher. However, subjects might need more time to turn on the switch with a larger number of epochs' smoothing. Considering the trade-off between the speed and accuracy, we determined 3 epochs for estimating a smoothed ERD_R feature to detect 'Intentional Control' and reject detection in 'No Control' state. The comparison of 3 epoch event-related moving average detection (a) online performed by S2 in session 5 and the simulated single power detection without moving average (b) is illustrated in Fig. 4. Two false positive detections using single power detection were avoided by 3 epoch moving average.
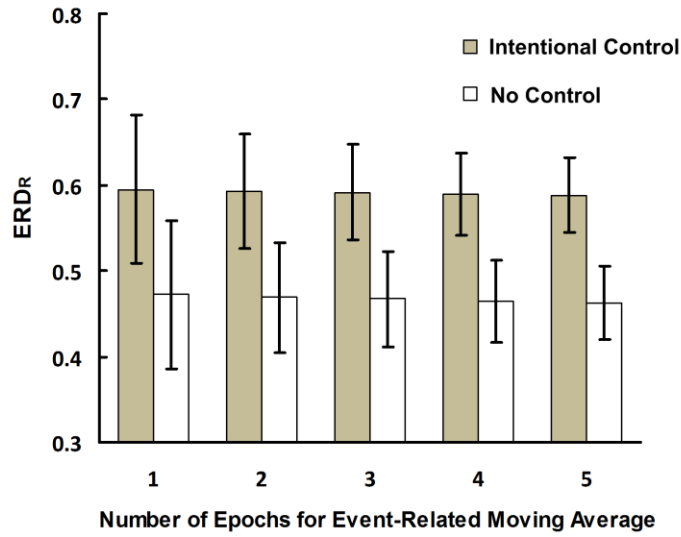
19

Fig. 3. The relative ERD, i.e. ERD_R statistics of subject S1 obtained from different numbers of consecutive epoch power smoothing. The ERD_R features were consecutively smoothed by moving average of past 1 to 5 epochs extracted from time window between high and low pitch sounds or time 0 to 1 shown in Fig. 2. The smoothed ERD_R sample mean and standard deviation was calculated from the data of one imagery session. As the sample mean of the smoothed ERD_R was equivalent to the grand average of ERD_R, the mean of the smoothed ERD_R was identical for different number of moving average. The variance/standard deviation of the ERD_R samples was reduced through a lager number of consecutive power moving average, that the variance of the 5 epochs smoothed ERD_R samples had the smallest variance. For both 'Intentional Control' and 'No Control' state, the reduced sample variance with a larger number of smoothing was observed. With 3 epochs smoothing, there was no overlapping of the sample standard deviation between 'Intentional Control' and 'No Control' state.

20
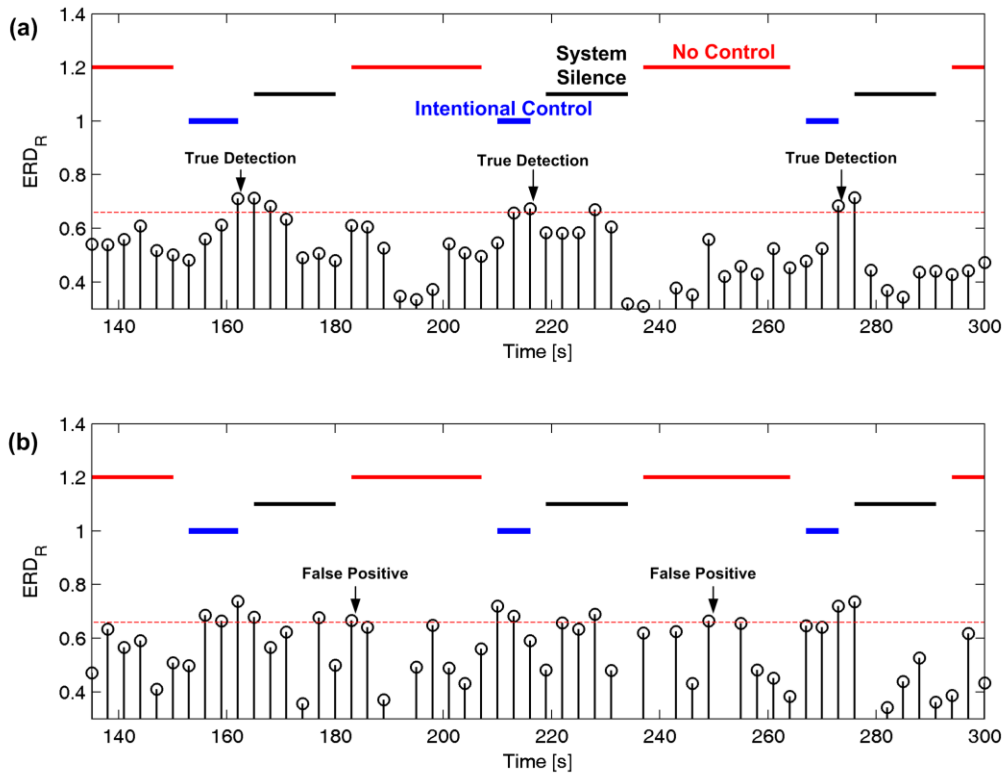
Fig. 4. An example of the relative ERD estimated from event-related moving average; (a) 3 consecutive epochs averaging obtained from online experiment; (b) signal power estimation without event-related averaging obtained from offline calculation. Through the smooth estimation by event-related averaging, two false positives in single power estimation were avoided. The proposed event-related moving averaging may effectively reduce the false positive rate in 'No Control' state.

21

3.3 Brain-controlled switch performance

We performed a multi-session online study to test the reliability and robustness of the brain-controlled switch performance during long-time operation. In the multi-session study, subjects performed active urging followed by motor imagery of finger movement. No physical movement was produced. The performance of the brain-controlled switch in the multi-session study with motor imagery is shown in table 1. Subjects were asked to successfully turn on the switch 10 times during one session. The average time of one session from all subjects was about 20-25 minutes. The total duration of the five sessions study was about 3-4 hours.

During the five sessions study while subjects were operating the brain-controlled switch, the computer continuously made detection every 3 s to determine whether the subjects intended to turn on the switch, though the switch was not responded during 'System Silence' even a positive detection was made. There were about 1 or 2 false detections out of around 160 prediction during the 'No Control' state for a single session, and the *FPR* was the percentage of the false positive detections made from total detections during the 'No Control' state. Zero FPR was achieved in some sessions for every subject. The overall false positive rate was 0.8% ±0.9% among all subjects. The urging time varied between 5.0 s and 27.7 s. The overall active urging time was 12.3 ±4.4 s for all subjects. The average FPR for all the subject was 0.70% in session 1; 0.43% in session 2; 1.0% in session 3; 0.90% in session 4 and 0.85% in session 5. There was no significant difference among the five sessions through one-way analysis of variance (ANOVA), $F_{(4,7)}=0.21$, p-value=0.927, alpha=0.05. Similarly, the average number of attempts to turn on the switch for all subjects was 16 in session 1; 14.5 in session 2; 11.8 in session 3; 10.8 in session 4

and 8.8 in session 5. There was no significant difference among the five sessions through one-way analysis of variance (ANOVA), $F_{(4,7)}=0.68$, p-value=0.629, alpha=0.05. Subjects achieved different performance in the operation of the brain-controlled switch; S1 made lowest mean FPR of 0.4%, and S4 made highest mean FPR of 1.2%. S1 also achieved shortest mean active urging time of 6.8 s and S3 needed longest mean active urging time of 16.9 s to turn on the switch.

Table 1 The online performance of brain-controlled switch with motor imagery during multi-session operation

	S1		S2		S3		S4	
	FPR [%]	UT (RT)[s]	FPR [%]	UT (RT)[s]	FPR [%]	UT (RT)[s]	FPR [%]	UT (RT)[s]
Session 1	0.0	6.7 (20.2)	0.0	22.0 (66.0)	1.8	13.1 (39.2)	1.0	22.2 (66.6)
Session 2	0.0	7.8 (23.3)	1.7	15.1 (45.2)	0.0	27.7 (83.0)	0.0	7.0 (21.0)
Session 3	2.1	7.1 (21.3)	0.0	8.4 (25.1)	0.9	17.4 (52.3)	1.0	14.8 (44.5)
Session 4	0.0	6.5 (19.5)	1.8	5.6 (16.7)	0.0	17.1 (51.4)	1.8	12.9 (38.8)
Session 5	0.0	6.1 (18.3)	0.9	5.0 (15.0)	0.0	9.1 (27.2)	2.5	14.9 (44.6)
Mean±SD	0.4±0.9	6.8±0.6 (20.5±1.9)	0.9±0.9	11.2±7.2 (33.6±21.7)	0.6±0.8	16.9±6.9 (50.6±20.8)	1.2±0.9	14.4±5.4 (43.0±16.3)

In addition to the multiple sessions with motor imagery, one session with physical movement was also performed before the multi-session motor imagery study. Though the motor tasks performed in motor imagery session and physical movement session were different, the data for estimating ERD features was extracted from the same time period while subjects were urging to move when they were asked to turn on the switch. The FPR achieved in the physical movement session were 0.0%, 1.2%, 0.0% and 0.0% for subjects S1, S2, S3 and S4, respectively. The active urging time/response time needed to turn on

23

the switch was 13.4 s/(40.2 s), 7.2 s/(21.5 s), 5.6 s/(16.9 s), 11.4 s/(34.3 s), respectively, with mean and standard deviation of 9.4±3.6 s/(28.2±10.9 s). Though the mean active urging time (9.4 s) with physical movement was less than that with motor imagery (12.3 s), they were not statistically different considering that the standard deviation among subjects in sessions with physical movement was 3.6 s, and the standard deviation among subjects in sessions with motor imagery was 4.4 s.

3.4. Offline analysis for overall performance

As shown in Fig. 5, using the simple algorithm adopted in the online interactive brain-controlled switch, i.e., threshold detection of beta band activity (ERD) on electrode C3 with 3 consecutive moving average, the true positive rate was more than 60% with a false positive rate under 1%, or about 95% under a false positive rate of 5% according to different working points (thresholds), which were inline or better than the state-of-the-art self-paced or asynchronous BCIs. Without considering a particular false positive rate, we evaluated the overall performance by 10-fold cross-validation accuracy (simple threshold algorithm): 96.2 ± 1.8% or 14.4 bits/min, which was also inline or better than state-of-the-art binary BCIs. In the 10 'Intentional Control', subjects needed about 3.0 times of repeated motor imagery tasks or 9 s of the response time to activate the switch, where the false positive rate was under 1%.
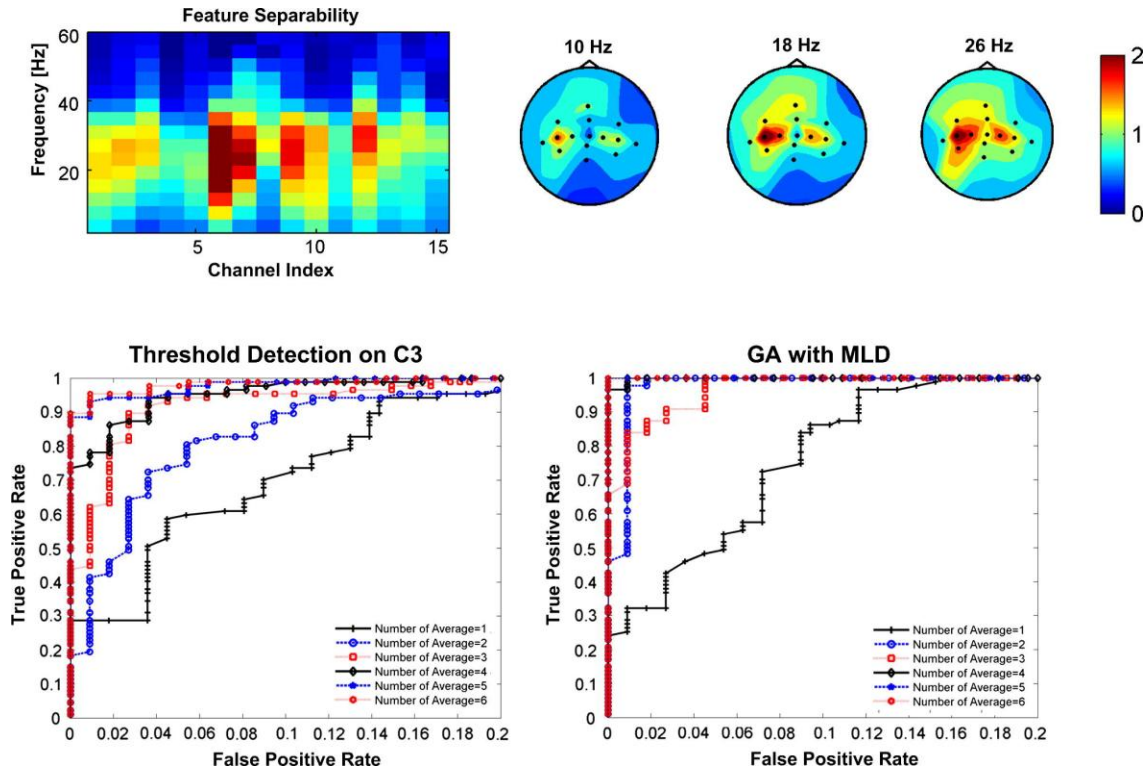
Fig. 5. Offline feature selection and classification from subject 2 under a modified motor imagery-based paradigm. The spatial and spectral features were indexed by Bhattacharyya distance: the central band from 15–30 Hz provided better separability. The computational intensive method using Genetic algorithm embedded with Mahalanobis linear distance classifier provided better detection rate in term of false positive rate and true positive rate than the simple detection on beta band frequency power on Laplacian derived channel C3. See detail in the text.

In order to test the improvement of performance using computation intensive method, feature selection method using feature ranking by Bhattacharyya distance (Bai et al., 2007) was employed. The best feature was central beta band from electrode C3 (Laplacian derived), which confirmed that the empirically determined feature for online interactive brain-controlled switch was adequate. According to the suggestion from a

25

self-paced BCI study (Fatourechi et al., 2008b), a genetic algorithm embedded by Mahalanobis linear distance (Marques, 2001) classifier was employed for classification: the 10-fold cross-validation accuracy (3 consecutive moving average) was $99.0 \pm 1.8\%$ or 18.2 bits/min, which was better than simple threshold algorithm ($96.2 \pm 1.8\%$ or 14.4 bits/min) as shown Fig. 5. Though the false positive rate and true positive rate were not much improved under none consecutive average, the true positive rate achieved 90% under false positive of 1%, which was greatly improved compared with the simple algorithm. The above result suggested that the performance of the proposed interactive switch can be further improved by employing better computational methods.

CHAPTER 4

Discussion

4.1 The event-related design of brain-controlled switch

For a real-world switch that may be used to turn on a light in a room, to detect a button click of a computer mouse, or in a variety of other applications, we are most concerned with the sensitivity (how easily we can activate the switch on one hand), and the specificity (that the switch is only activated when we intend to activate it on the other hand). Depending on the different purposes, a real-world switch can be designed either with high sensitivity or with low sensitivity so that the users may need to exert more effort or pay more attention to activate the switch thereby decreasing the possibility of the miss-operation. The specificity of a real-world switch is usually not as big of a concern because the common electrical or mechanical switch has a very low possibility of receiving random or unintended inputs that may accidentally activate the switch. Also, users will only attend to a real-world switch if and only if they need to activate it. Besides, users do not pay attention to the switch or think about its existence. Ideally, the brain-controlled switch should be as functional as a real-world switch, though the brain-controlled switch is operated by brain signal, whereas a real-world switch is usually operated by human hand. Unlike the hand operation which is usually very reliable,

27

developing a similarly reliable brain-controlled switch is much more challenging because brain signals usually have a very low S/N ratio which thereby makes brain signal-based operation unreliable. Thus, the greatest challenge in developing a brain-controlled switch is improving the S/N ratio of the brain signals for reliable operation. Concurrently, the brain-controlled switch should have similar properties with a real world switch, i.e., users may choose not to think about the switch unless they intend on using it.

In this study, we proposed a brain-controlled switch using the ERD feature associated with human natural motor control, i.e. motor imagery or motor execution. In contrast to common rhythm regulation-based BCI, users do not need long-term training to learn how to effectively and reliably regulate their brain rhythm because ERD is a natural physiological process. Being a natural physiological activity, ERD, however, usually has a large variance. This will lead to more difficulties in switch design because most of the time users do not want to activate the switch while they are at rest or performing a different task. The variance in ERD, therefore may very easily cause false operation or produce false positives that activate the switch without user intention. In order to improve the S/N ratio of the brain signal and reduce the possibility of false positive detection, we proposed a novel paradigm for an event-related brain-controlled switch in which we applied an enhanced ERD feature that was consecutively smoothed by moving average. From conventional spectral density estimation, the excessive variance in spectral density estimation may be reduced by enlarging the estimation window, that is to say, spectral density is estimated from a longer length of data (Proakis & Manolakis 2006). Therefore, a smoothed ERD with less variance can be obtained from a longer data window. In order to differentiate between 'Intentional Control' and 'No Control' states, users are required

to pursue longer motor imagery task during intentional control state. However, evidence from sport medicine shows that humans are unable to sustain prolonged motor imagery (Verbunt et al. 2008). Moreover, the sustained attention is a mentally intensive task which may cause fatigue. In Birch and his colleagues' study, one of four subjects participated in the study reported fatigue and was unable to finish 75 imagined movements (Birch, Bozorgzadeh & Mason 2002). Further, the fatigue from the sustained attention to perform motor imagery is a greater factor in paralyzed patients, such as those with amyotrophic lateral sclerosis (Sellers & Donchin 2006). In order to reduce the fatigue from steady-state active motor imagery tasks, we proposed an event-related design allowing the users to perform motor imagery of active urging for 1 s and then to relax for 2 s. The switch was interactive such that users might perform repeated motor imagery of active urging tasks with relaxation in between. This design is similar to a real-world switch that is not very sensitive, and is designed partly for reducing the possibility of random or unintended operation. Making repeated effort to activate the switch would be easier than steadily pushing the switch, which may induce muscle fatigue or even muscle pain if the action time is too long in one attempt.

EOG signal induced by eye-movement or blink may decrease asynchronous BCI based on low frequency activity that is overlapped with EOG activity (Noureddin, Lawrence & Birch 2008). As the detection for the proposed brain-controlled switch was determined by the event-related moving average of ERD in beta band, the eye-movement or blink didn't affect the detection performance, where subjects were not asked to intentionally reduce eye-movements and blinks. In the contrast shown in Fig. 2, we didn't

29

observe much difference in low frequency band between 'Intentional Control' and 'No Control'.

The effectiveness of the novel event-related switch design was demonstrated in this study. At first, similar to the real-world switch, the users did not perform any particular tasks when they were not instructed to turn on the switch. Though users did not perform any active control during 'No Control' state, the false positive rate was minimal (average about 0.8%) among the tested fours subjects with some subjects even achieving 0% false positive rate. A real-world switch is designed for long-term operation that is always ready and responsive whenever one may want to activate it. In this study we designed a multi-session experiment to test the reliability and robustness of the brain-controlled switch for long-term operation while also considering methods to decrease fatigue from motor imagery during long-term use. Moreover, no subject reported that they felt considerable fatigue after the prolonged multi-session study. The stable performance suggests that the proposed brain-controlled switch might be suitable for long-term use as a real-world switch.

4.2 Improvement of performance

In this study, we introduced the design of a brain-controlled switch with a novel paradigm. We employed a simple threshold method to differentiate the 'Intentional Control' from the 'No Control' state. The threshold for detection was determined by a rough, manual adjustment where we didn't apply an optimization method to adjust the threshold. We have achieved a minimal false positive detection rate with an acceptable active urging or response time to activate the switch. Comparing with a real-world switch, the response time to activate the switch is relatively longer for the brain-

30

controlled switch. Further efforts are required to increase the sensitivity of the brain-controlled switch in order to reduce the response time without sacrificing the false positive rate. We expect that the performance of the proposed brain-controlled switch can be further improved by employing more computationally intensive classification methods with optimization such as support vector machine as suggested by pervious BCI approaches (Lal et al. 2004; Fatourechi, Ward & Birch 2008b) as well as effective feature selection methods such as genetic algorithm (Raymer et al. 2000; Gupta & Palaniappan 2007) to determine optimal EEG channel and frequency band for detection. In additional to employment of computationally intensive methods, we expect that a better performance can be achieved by exploring a new feature to improve detection accuracy such as a post-motor activity of ERS (Pfurtscheller & Solis-Escalante 2009). Another factor requiring optimization is the number of epochs for consecutive moving average to obtain a smoothed ERD feature. A larger number for epochs may provide a more smoothed ERD; however, the sensitivity to activate the switch may be reduced that subjects may require a longer time period to activate the switch. Further, the behavioral performance during active urging following with motor imagery might also pose an important factor for consideration. Subject 4 had a stronger ERD when urging to move before actual physical movement, however, he had a reduced ERD during the urge before motor imagery of the movement. This subject also reported difficulty with urging a movement followed by the actual movement. Therefore, appropriate instruction to perform an active urge should also be considered in future study. Through the above optimization, we expect that the proposed brain-controlled switch can serve as a plausible real-world switch that users may operate solely with their 'mind'.

31

Part 2   Nerve Conduction Study Simulator Software Design

CHAPTER 5

Introduction

5.1 Neuron action potential

Neuron action potential, also known as "nerve impulse" and "spike" plays a central role in neural cells network communication, like the digital signal transmitted in man-made communication network, and in human motor function as it causes the muscle contraction in neural muscular junctions.

A resting membrane potential established across the cell membrane enable neurons to respond to stimuli and conduct impulses. The dynamics of sodium and potassium channels' open and close in the membrane caused by stimuli give the shape of the action potential, as shown in Fig. 6. The conduction speed of the impulse along neuron fiber is determined by radius of the fiber and presence and absence of myelin.
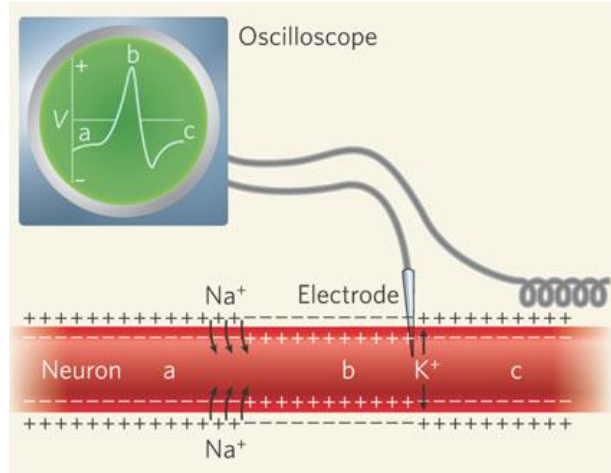
Fig. 6. Neuron action potential

(http://people.eku.edu/ritchisong/301notes2.htm)

5.2 Nerve conduction study

A nerve conduction study (NCS) is a neurological test used to evaluate the electrical conduction properties, in terms of latency, amplitude and conduction velocity, of the nerves of the human body.

The nerve conduction study is performed by placing surface stimulus electrodes and recording electrodes over the nerve one intends to study, the stimulus electrodes give small electrical stimulus and recording electrodes will pick up the electrical impulse conducted along the nerve. Recording electrodes are placed along sensory or mixed nerves in sensory nerve study. While in motor nerve study, recording is from the muscle being innervated by motor nerve. The waveform of the electrical impulse will be recorded; latency and amplitude of the recorded electrical impulse will also be measured and displayed along with the waveform by nerve conduction study equipment. After stimulus several points along the nerve, nerve conduction velocity can be calculated for each stimulating segment.

33

The nerve conduction study can provide physician with the information of latency, amplitude and conduction velocity of the nerve in determining the types and positions of the nerve dysfunction, since nerve conduction parameters have standard ranges in normal condition.

So, the nerve conduction study is an important neurology test. It is often done to aid in diagnosing various diseases that impact the nerves, distinguish between muscle and nerve disorders, and monitor if a nerve is recovering from injury.

5.3 Motivation

5.3.1 Simulation in health care

As simulation has achieved big success in personnel training for aviation, nuclear power and military fields, simulation in health care is also undergoing dramatic changes in recent decade. Sharing the properties of intrinsic hazard and complexity with health care, but the low failure rate management in those industries gives huge impetus to apply simulation techniques in health care to reduce patient risk and improve patient care. The simulation in health care is also described as "flight simulation for doctors"(Gordon, Oriol & Cooper 2004).

Simulation is a technique to replace and amplify real experiences through imitating critical aspects of the real world in an interactive way. Simulation used in health care is the devices that provide a simulated patient or part of a patient and appropriate responses to the simulation participants' actions(Gaba 2004). Through the simulation, participants are able to make mistakes and learn from the mistake without any risks to patient. More importantly, the scenarios related to the known error producing conditions can also be created in the simulated environment to enhance the learning. Evidence

34

showed simulation participates may understand and retain the complex information more efficiently than the traditional methods(Gordon et al. 2003). Therefore, simulation may reduce medical error by the improvement of medical personnel's knowledge understanding, skills and experience. In addition, simulation allows the medical educator to provide reproducible curriculum for all students and more hands on experience at the knowledge studying phase compared to traditional teaching.

Driven by the demand in health care education and rapid technology development, simulator used in the health care also evolves a lot. In 1960s, a mannequin for training in mouth to mouth ventilation was developed. An internal spring was attached to the chest wall to simulate the cardiac compression in the mannequin. Not computer driven, not breathing and lacking a heartbeat, the simulator has been widely used for CPR training. Later, Harvey, a life-sized patient simulator was created with abilities to display many physical findings like palpation, auscultation, and electrocardiography. It was capable to simulating many cardiac diseases by varying those physiological variables. With the computer and information technology, the high-fidelity patient simulators by far can breathe, talk, blink, displays electrophysiological signals placed in a real operating room, surrounded by actual equipment and even response to dosage based on physiology and pharmacology models.

Although there is no strict proof of the benefits of simulation training in health care, the potential benefits and cost of the simulation attracts more and more health institutes. The number of medical simulation centers rising from under 20 to over 200 in less than a decade. The high-tech simulator will promise a revolutionary role in medical education(Friedrich 2002).

5.3.2 Simulator for Nerve Conduction Study

The techniques associated with nerve conduction study are not easy to learn and to perform. These techniques require the physician to recognize nerve position and correct stimulation points for each study, and to recognize specific electrical response waveform related to each study. The response waveform is sensitive to the position of stimulus. The amplitude of the waveform will drop dramatically, when the stimulus point is off the nerve, while these parameters of response waveform, such as amplitude, latency and conduction velocity, provide physician important information in diagnosing.

Current training methods have required that the physicians learn these procedures by observation and by practicing the procedures directly on patients or healthy volunteer subjects. Although the stimulus is a small low-voltage current, the repeated trial-error learning process of novice physician will inevitably cause intense tingling sensation and muscle twitching of the human subjects.

Accordingly, the motivation of this study is to design a nerve conduction study simulator which can be used to train physicians to perform the study with more confidence and experience, especially for those making transition from theory to performing the techniques on human subjects.

36

CHAPTER 6

Nerve Conduction Study Simulator Software Design

6.1 Nerve Conduction Study Simulator

Nerve conduction study simulator is a medical simulator designed to teach novice physician and refine their skills in conducting nerve conduction study test. The components of the simulator are shown in Fig. 7. The simulator in this thesis is used to simulate nerve conduction study of upper limb.
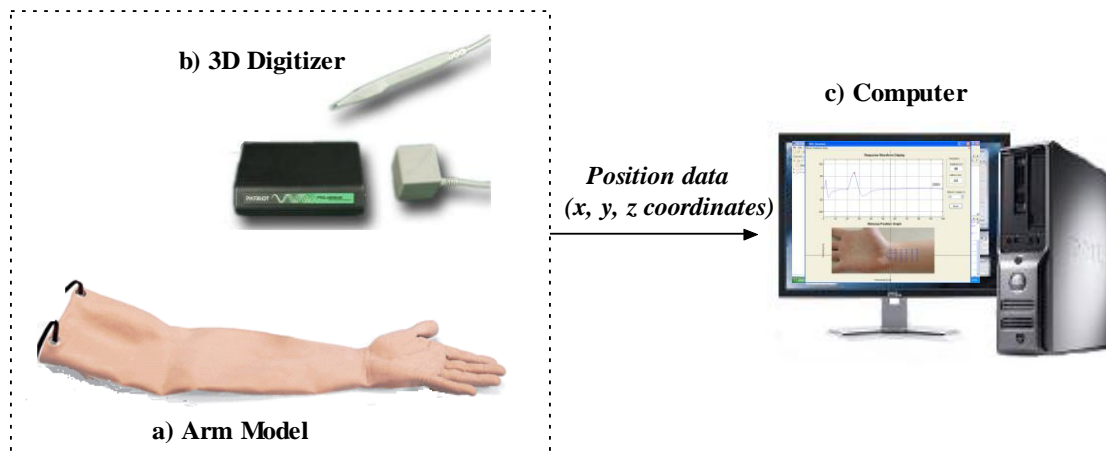

Fig. 7. Nerve Conduction Study Simulator System. The system consists of a) An arm model, b) 3D digitizer, used to simulate the stimulation electrode (cathode), c) A computer, used to calculate and display response wave form based on stimulation position input.

As shown in Fig. 7, a physician can use 3D digitizer pen as stimulation electrode (cathode) to touch the desired stimulus site of a certain study, assuming reference and recording electrodes are placed correctly according to the study. The coordinates of touched stimulus site are sent to computer simulator program. Then a typical response waveform corresponding to this stimulus site is calculated and displaced on computer screen.

6.2 Design of Nerve Conduction Study Simulator Software

The software of nerve conduction study simulator maps stimulus site coordinates on the arm model to a response waveform corresponding to this site based on typical parameters of nerve being studied and waveform generation model, as shown in Fig. 8.
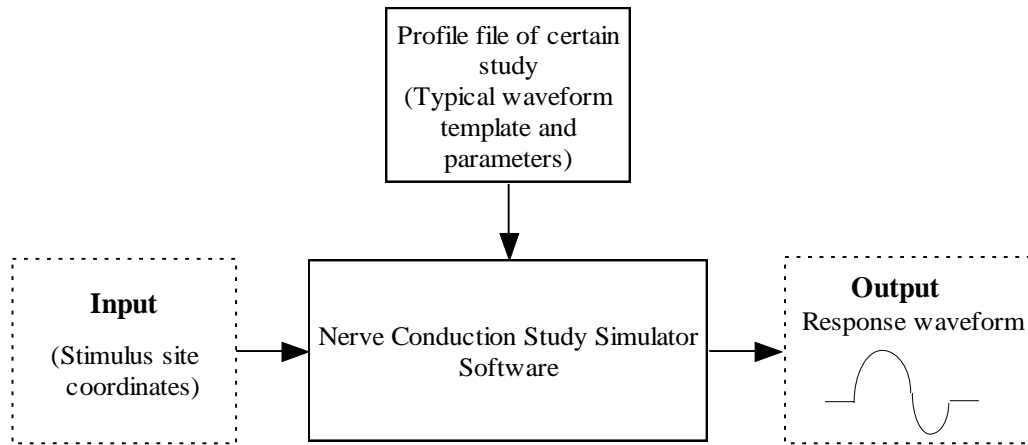

Fig. 8. Function of nerve conduction study simulator

38

6.2.1 Waveform parameters

Latency and amplitude are two critical parameters in characterizing the response wave form, as in Fig. 9. They are defined as following(Hang J. Lee 2004):
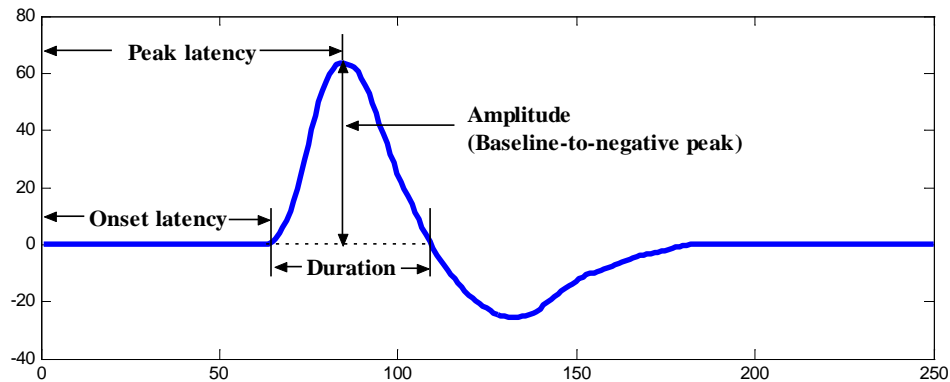

Fig. 9. Waveform Parameters

Latency time (ms) for motor responses is measured from the shock artifact to the initial negative defection of the response from the baseline of the video display. Latency time equals to onset latency as shown in Fig. 9. The amplitude in millivolts(mV) is measured from the baseline to the initial positive dip of the motor response.

Latency time (ms) for sensory responses is measured from the shock artifact to the peak of the initial negative deflection (upward). Latency time equals to peak latency as shown in Fig. 9. The amplitude in microvolts (μV) is measured from the baseline to the initial positive dip of the motor response.

Another important parameter nerve conduction velocity is calculated by measuring the distance (mm) between two stimulation sites and dividing by the

39

difference in latency (ms) from proximal stimulus and the latency (ms) of the distal stimulus, as in formula 3.

$$conduction\ velocity\ (m/s) = \frac{distance\,(mm)}{proximal\ latency\,(ms) - distal\ latency\,(ms)} \quad (3)$$

6.2.2 Standard stimulation point and template waveform.

Standard stimulation point is the convention stimulation site used by neurology physician and in nerve conduction study textbook, which provides the normal response waveform parameters for reference. For example, in median sensory conduction study the standard stimulation site S (stimulation electrode cathode position) is measured from recording electrode R1 to the wrist in a distance of 13 cm, as shown in Fig. 10. In normal condition amplitude of the response waveform is larger than 15 μV and latency should be smaller than 3.7 ms.
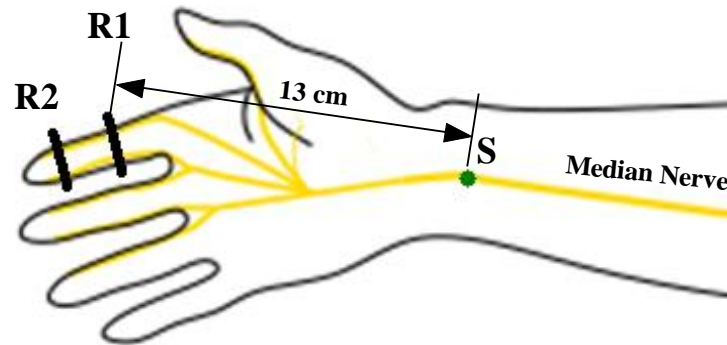
Fig. 10. Standard stimulation site of median sensory nerve study.

R1 is the recording electrode. R2 is the reference electrode. S is the cathode of the stimulation electrode.

The template waveform consists of a flat base line and deflection waveform extracted from real experiment data from VCU Medical Centre EMG Lab. The latency and amplitude of template wave from are adjusted according to real experiment response waveform parameters by time shifting and magnitude scaling. The template waveform represents the response waveform at the standard stimulation point. The template waveform of median sensory study is shown in Fig. 11, with parameters (amplitude 65 µV, latency 3.5 ms) measured from real experiment.
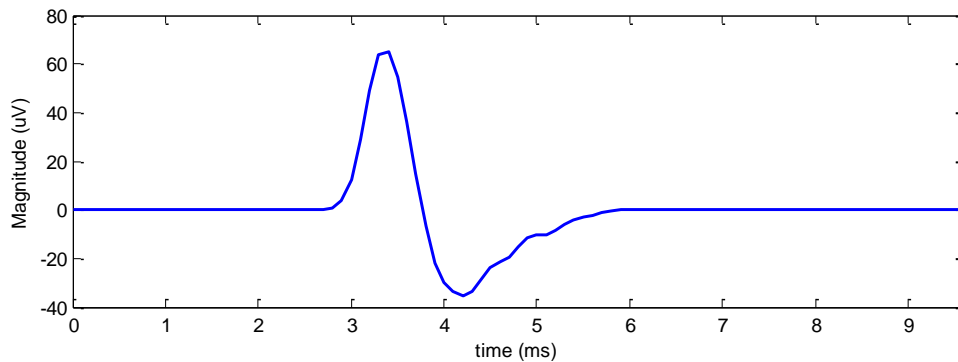

Fig. 11. Template waveform of median nerve study

(Amplitude = 65 µV, latency = 3.5 ms)

6.2.3 Waveform generation model within study region

The nerve conduction study simulator program calculates response waveform corresponding to the new stimulation site based on waveform generation model. The waveform generation model follows two principles that determine latency and amplitude of new response waveform(David C. Preston 2005). 1) As a 1cm distance new stimulation point move away from standard stimulation site along the nerve being studied, the latency will increase (move opposite recording electrode direction) or decrease 0.2 ms;

41

2) As stimulation point move vertically offside the nerve direction, the amplitude will decrease. From the experiment test data, we assume here the amplitude will decrease to one half of its original size as the vertical distance increase every 0.5 cm.

For example, in median nerve sensory study, the electrodes placement is shown in Fig. 12. S is standard stimulation point. N point is 1cm away from S along nerve direction. $\overrightarrow{SN}$ vector is defined as nerve direction vector. S' is the new stimulation site. The distance from S' to standard point S along the nerve direction is $a = \overrightarrow{SS'} \bullet \overrightarrow{SN}$ (cm). The vertical distance away from the median nerve is $b = \sqrt{\left|SS'\right|^2 - a^2}$ (cm). Assume waveform of the standard stimulation site is represented by function w(t) with standard latency L, and amplitude A. So, following the principles, the latency shift LT can be expressed by LT (a) = 0.2*a (ms); the amplitude change will be $A(b) = \left(\dfrac{1}{2}\right)^{2b}$ times of template waveform amplitude.

The waveform of the new stimulation site can be expressed as function f(t) as formula 4.,
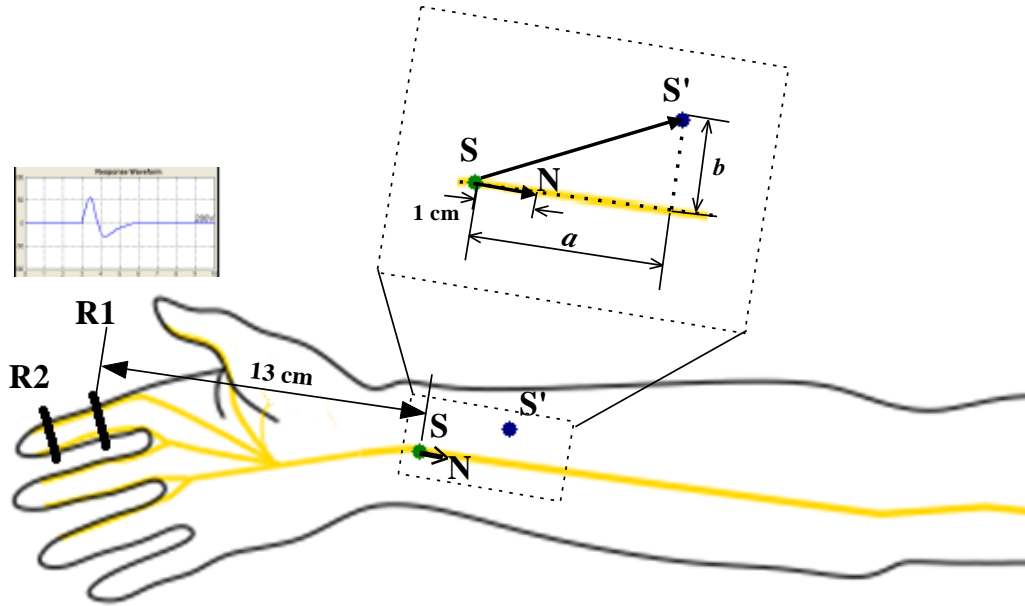
$$f(t) = A(b)w(t + LT(a)) \tag{4}$$

Fig. 12. Median nerve sensory study configuration. R1 is recording electrode, R2 is reference electrode, S is the position of standard stimulation point. It is 13 cm from R1. S' is new stimulation site. N point is 1cm away from S along nerve direction.

Study region is the small area around stand stimulation point where the waveform model works to generate an approximation waveform to simulate the real study test, as the dot lined square in Fig. 12. When stimulation point is outside this region, a message "out of study region" will be displayed on the screen.

6.2.4 Study profile

Study profile is a data file containing information of standard stimulation point coordinates, nerve direction vector, waveform template and study region boundary for each study. Waveform generation model calculates waveform according to formula 4 based on values from this file for each stimulation point input of a nerve conduction study. Therefore, standard point coordinates, nerve direction vector and waveform

43

template are three key components for waveform generation model of each nerve conduction study.

Before taking arm position picture of each study, a standard point of the study and point of 1cm away along the nerve were marked by experienced doctor. In software setup phase, the coordinates of the standard points, nerve direction vector and boundary coordinates of the arm position picture for each study can be acquired by mouse selection.

6.2.5 Graphic User Interface Design for Nerve Conduction Simulator

Through the graphic user interface, user interacts with the simulator in the software simulation stage. There are four main parts on the interface as shown in Fig. 13. The first is study selection region contains study selection button that user can switch between different nerve study. The simulation software provides 10 nerve conduction studies of upper limb. They are Median Sensory Study, Ulnar Sensory Study, Median Palmar Study, Ulnar Palmar Study, Radial Sensory Study, Median Motor Study, Ulnar Motor Study, Lateral Antebrachial Cutaneous (LAC) Study, Medial Antebrachial Cutaneous (MAC), and Dorsal Ulnar Study. The second is arm position display region in which the arm picture for current study is showed. In the software simulation stage, the stimulation point coordinates input is from the arm picture. A standard stimulation point was marked by yellow point in each arm picture of different study. User can click at different positions around the stimulation point of the arm picture by computer mouse to simulate stimulating at different site on the arm in real study. Once a left click of the mouse at the point on the arm picture within the study region of current study is detected, the response waveform will be displayed in the waveform display region which is the third part of the interface. The response waveform is calculated from the stimulation

44

point coordinates of the arm picture based on waveform generation model and study profile data. The last part of the interface is parameters display region. It will display values of latency and amplitude associated with each response waveform.
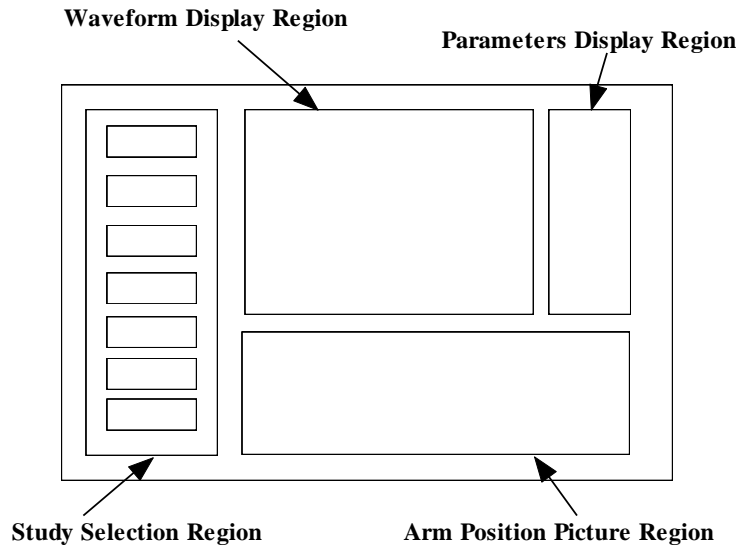

Fig. 13. Framework of Nerve Conduction Study Simulator Software interface

Matlab is used to create the nerve conduction study simulator GUI, since it is a powerful computing platform and the GUI program can be easily created by GUI guide. The final simulator user interface is as Fig. 14.
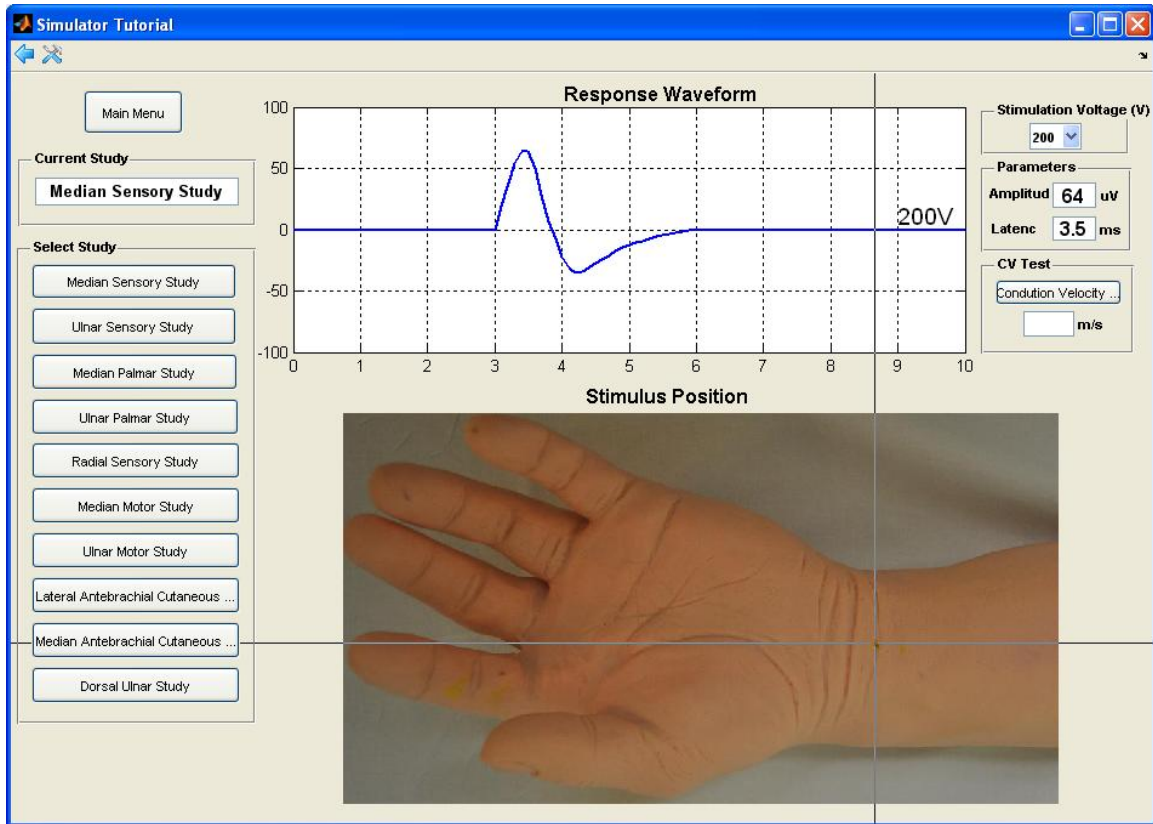
Fig. 14. Graphic User Interface Implemented by Matlab

6.2.6 Implementation of the Nerve Conduction Study Simulator Software Interface

The procedures of Nerve Conduction Study Simulator Software Interface implementation is shown by the flow chart in Fig. 15. Once a study is selected by clicking the button of that study, the arm picture for the study is shown in arm position picture region. The profile date of the study is read by program. A number is assigned to study flag variable of the program to identify current study. Then after the initialization, the program is at the stage waiting for stimulation input. If user clicks a stimulation point within the study region on the arm picture, the coordinates of the stimulation site is passed to waveform generation model to calculate response waveform from the input and

46

profile data of current study. Finally, the response waveform is displayed at the waveform display region. Parameters of the response waveform (latency and amplitude) are also displayed at the parameters display region. And the program returns to the stage of waiting for new stimulation input.
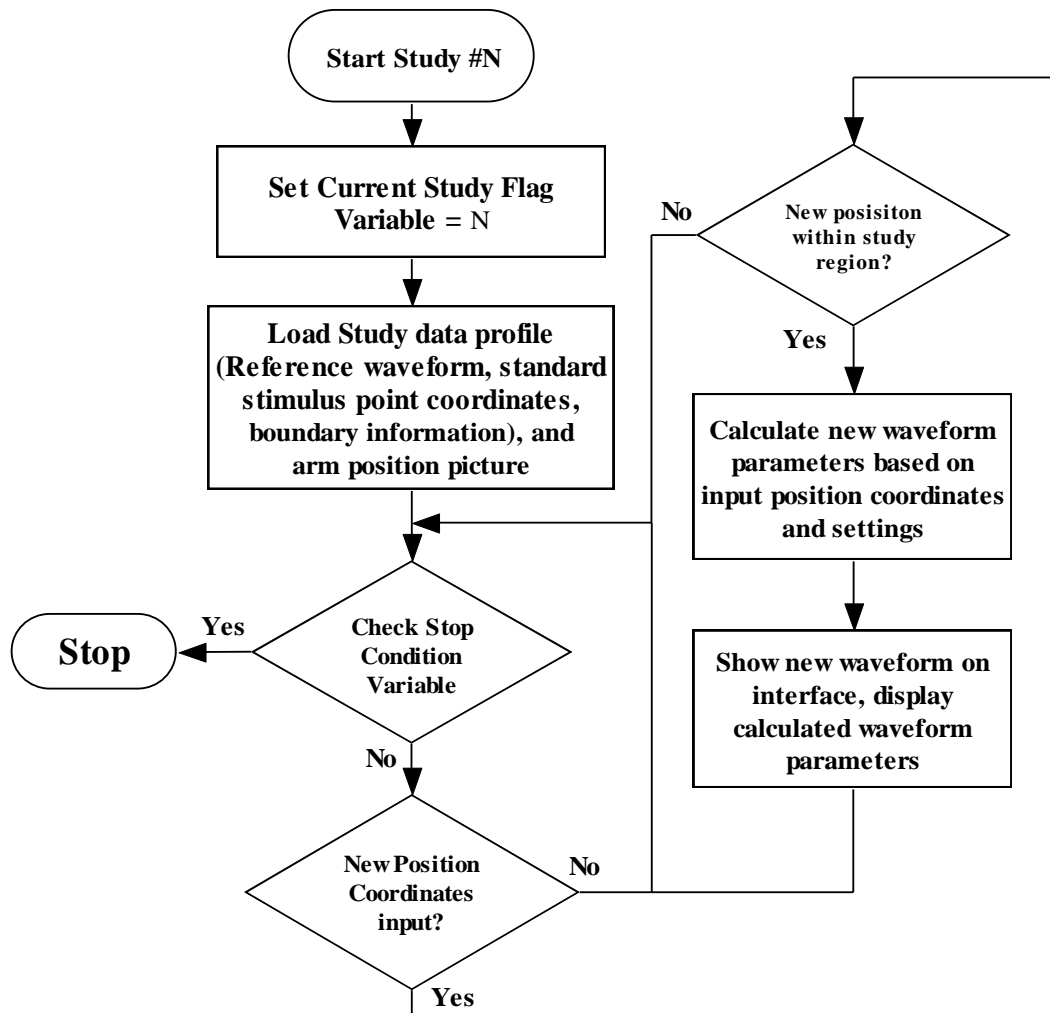

Fig. 15. Flow chart of a nerve conduction study

6.2.7 Nerve conduction velocity test in simulation software

In median motor study and ulnar motor study, the simulation software provides nerve conduction velocity test function. To perform conduction velocity test user clicks conduction velocity test button in parameters display region on interface. User stimulates

47

at the first stimulation sites. The response waveform will be displayed in waveform display region as in nerve conduction study discussed above. Then user stimulates at the second stimulation sites. Nerve conduction velocity of the segment will be shown in parameters display region on the interface based on the distance between two stimulation sites and latency difference of the two sites as described in formula 3. In median motor study the distance between standard stimulation site at wrist and standard stimulation site at elbow measured from real experiment is 240 mm. In ulnar motor study, the distance between standard stimulation site at wrist and standard stimulation site below elbow is 240 mm. the distance between standard stimulation site below elbow and stimulation site above elbow is 140 mm.

The program flow chart of nerve conduction velocity test is shown in Fig. 16. The conduction velocity test starts by clicking the conduction velocity button. Program then checks current study. If current study is not median motor or ulnar motor study, the conduction velocity test will stop and a message will be displayed on the interface. If current study is median motor or ulnar motor study, the program will load its study profile data. After initialization program enters stage waiting for two stimulation points input. Once two stimulation points input is detected, then nerve conduction velocity is calculated based on formula 3 and displayed in parameters display region. Then conduction velocity test stops.
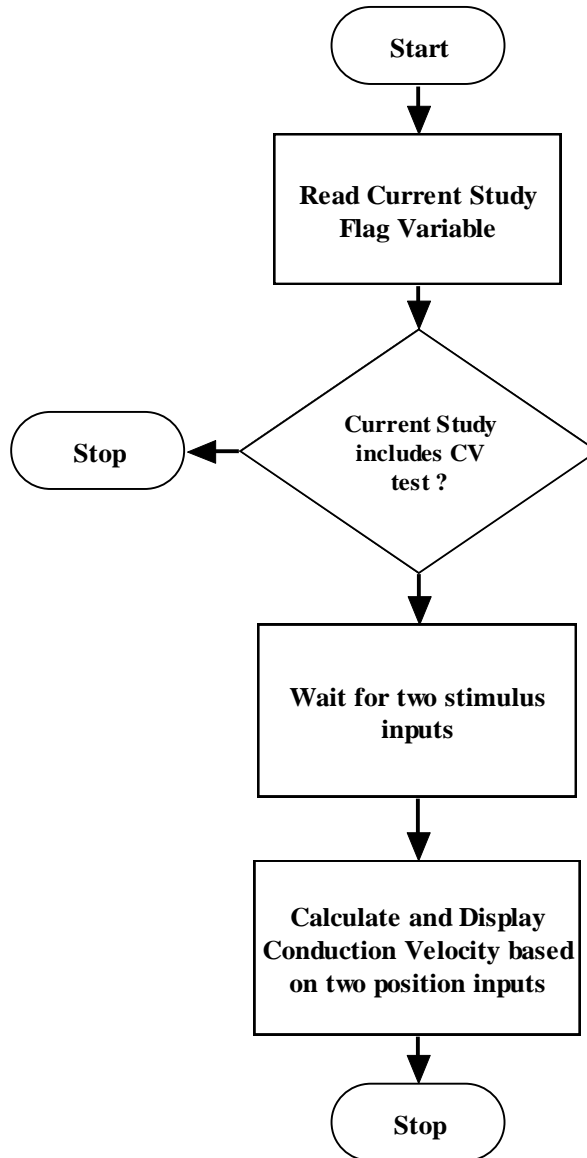
48

Fig. 16 Flow chart of nerve conduction velocity test

6.3 Expanding to include pathological conditions

Since each simulation study is defined by a standard stimulation point, nerve conduction vector, and waveform template, the normal parameters of each study can be changed to those of the pathological condition to demonstrate what the response waveform would look like approximately in different pathological conditions. The pathological conditions being included in the simulation software are mild carpal tunnel syndrome, moderate carpal tunnel syndrome, sever carpal tunnel syndrome, ulnar neuropathy at the wrist, ulnar neuropathy at the elbow, distal axonal sensory neuropathy, distal demyelinating sensory neuropathy, distal sensory motor neuropathy, and median nerve neuropathy with conduction block at the forearm. The typical parameters of those pathological conditions for each study are shown in table 2. The pathological condition scenarios are incorporated in case study mode in simulation software. They are numbered from case 1 to case 9. When user selects a case study, the pathological condition name is not provided. User has to practice on the 10 nerve conduction studies of the upper limb nerves on the simulation software to make a judgment, what current pathological condition it is, based on knowledge and observations. The judgment can be checked by clicking the answer button, on interface in case study mode, which will show the name of current pathological condition. The case study mode of simulator adds a very meaningful aspect in nerve conduction study simulation training.

Table 2 Amplitude and latency parameters for 9 pathological conditions

	Mild Carpal Tunnel Syndrome	Moderate Carpal Tunnel Syndrome	Severe Carpal Tunnel Syndrome	Ulnar Neuropathy at the Wrist	Ulnar Neuropathy at the Elbow	Distal Axonal Sensory Neuropathy	Distal Demyelinating Sensory Neuropathy	Distal sensory motor Neuropathy	Median Nerve Neuropathy with Conduction Block at the Forearm
Ulnar Palmar Sensory Study	Normal	Normal	Normal	Latency: 2.5	Latency: 2.5	Amplitude: 9	Latency 3.2	Amplitude: 9 Latency: 3.2	Normal
Median Palmar Sensory Study	Latency: 2.6	Latency: 2.8	Latency: 2.9 Amplitude:25	Normal	Normal	Amplitude: 31	Latency: 3.2	Amplitude: 31 Latency: 3.2	Normal
Ulnar Sensory Study (Rings)	Normal	Normal	Normal	Latency: 3.4	Latency: 3.5	Amplitude: 4	Latency: 4.0	Amplitude: 4 Latency: 4.0	Normal
Median Sensory Study (Rings)	Latency: 4.0	Latency 4.1	Latency: 4.3 Amplitude 12	Normal	Normal	Amplitude: 7	Latency: 4.5	Amplitude: 7 Latency: 4.5	Normal
Radial Sensory Study	Normal	Normal	Normal	Normal	Normal	Amplitude: 10	Latency: 3.0	Amplitude: 10	Normal
Ulnar Motor Study	Normal	Normal	Normal	Latency: 4.0	Proximal Latency: -Amplitude drop: 15% -CV drop	Normal	Normal	Latency: 4.7 CV : 33	Normal
Median Motor Study	Normal	Normal	Distal Latency: 5.3	Normal	Normal	Normal	Normal	Latency: 5.9 CV : 33, 32	Distal Amplitude: 12 Proximal Amplitude: 8

(According to the study name in the first column of the table, the latency refers to peak latency in the sensory study, while the latency refers to onset latency in motor study.)

CHAPTER 7

Conclusion and Future work

As an education and training tool, the nerve conduction simulation software provides the function to simulate 10 different nerve conduction studies in normal and 9 pathological conditions of the upper limb. It shows a typical response waveform when stimulating at standard stimulation point of the study. When stimulation sites move away along the nerve being studied in the small area around standard stimulation point, the latency of response waveform increases. When stimulation sites move offside the nerve in the small area around standard stimulation point, the amplitude of response waveform decreases. The variations of response waveform at different stimulation sites and under different pathological conditions in the simulation practice can help physicians in finding optimal stimulation site of different nerve conduction studies and in enhancing their knowledge of pathological condition influence on different nerve conduction study.

The nerve conduction simulator software is designed to easily incorporate new study and easy to interface with external hardware. Since the waveform generation model only requires standard stimulation point coordinates and nerve direction vector and waveform template from real experiment data, a new study can be easily created by providing these data to approximately simulate the response waveform around the standard stimulation point within a small area. Also, once a stimulation position

52

coordinates input is detected either from cursor position data from software simulation or from the 3D digitizer position data from physical arm model, the response waveform of the new stimulation site will be generated by waveform generation model.

The nerve conduction study simulator consists of both software and hardware part. The future work may extend to incorporate 3D digitizer into the system. We need to find a product that provides good support and tools for custom software development. Current software is developed on Matlab, so interface software need to be developed to read the hardware position output and send the information to the application software. In addition, a fixture mechanism for the dummy arm and 3D digitizer is also needed to provide a fixed physical coordinate system that is consistent with the software molder coordinate system.

Important software improvement can also be done to provide better user training experiences. For example, the case study section can be designed more realistically and detailed. It may include a case debrief section displaying detailed patient information on medical history and symptoms. The user will be asked to practice through the simulation study to make a judgment. The results of other further test may also be provided to assist the user in decision making. The interface design can be designed more interactively and can simulate the process more like a patient visit.

Since nerve conduction study on the upper limb is just a fraction of the study, based on successfully connected the hardware to the system and more interactive software design, the simulator may expand to other body parts such as facial part and leg part.

53

Literature Cited

Literature Cited

Bai, O, Lin, P, Vorbach, S, Li, J, Furlani, S & Hallett, M 2007, 'Exploration of computational methods for classification of movement intention during human voluntary movement from single trial EEG', *Clin Neurophysiol*, vol. 118, no. 12, pp. 2637-55.

Bashashati, A, Mason, S, Ward, RK & Birch, GE 2006, 'An improved asynchronous brain interface: making use of the temporal history of the LF-ASD feature vectors', *J Neural Eng*, vol. 3, no. 2, pp. 87-94.

Birch, GE, Bozorgzadeh, Z & Mason, SG 2002, 'Initial on-line evaluations of the LF-ASD brain-computer interface with able-bodied and spinal-cord subjects using imagined voluntary motor potentials', *IEEE Trans Neural Syst Rehabil Eng*, vol. 10, no. 4, pp. 219-24.

Birch, GE & Mason, SG 2000, 'Brain-computer interface research at the Neil Squire Foundation', *IEEE Trans Rehabil Eng*, vol. 8, no. 2, pp. 193-5.

David C. Preston, BES 2005, *Electromyography and Neuromuscular Disorders: Clinical-Electrophysiologic Correlations*, 2 edn, Elsevier Health Sciences.

Faradji, F, Ward, RK & Birch, GE 2009, 'Plausibility assessment of a 2-state self-paced mental task-based BCI using the no-control performance analysis', *J Neurosci Methods*, vol. 180, no. 2, pp. 330-9.

Fatourechi, M, Ward, RK & Birch, GE 2008a, 'Performance of a self-paced brain computer interface on data contaminated with eye-movement artifacts and on data recorded in a subsequent session', *Comput Intell Neurosci*, p. 749204.

Fatourechi, M, Ward, RK & Birch, GE 2008b, 'A self-paced brain-computer interface system with a low false positive rate', *J Neural Eng*, vol. 5, no. 1, pp. 9-23.

Friedrich, MJ 2002, 'Practice makes perfect: risk-free medical training with patient simulators', *JAMA*, vol. 288, no. 22, pp. 2808, 2811-2.

Gaba, DM 2004, 'The future vision of simulation in health care', *Qual Saf Health Care*, vol. 13 Suppl 1, pp. i2-10.

Georgopoulos, AP, Schwartz, AB & Kettner, RE 1986, 'Neuronal population coding of movement direction', *Science*, vol. 233, no. 4771, pp. 1416-9.

Gordon, JA, Oriol, NE & Cooper, JB 2004, 'Bringing good teaching cases "to life": a simulator-based medical education service', *Acad Med*, vol. 79, no. 1, pp. 23-7.

Gordon, JA, Tancredi, DN, Binder, WD, Wilkerson, WM & Shaffer, DW 2003, 'Assessment of a clinical performance evaluation tool for use in a simulator-based testing environment: a pilot study', *Acad Med*, vol. 78, no. 10 Suppl, pp. S45-7.

Gupta, CN & Palaniappan, R 2007, 'Enhanced detection of visual-evoked potentials in brain-computer interface using genetic algorithm and cyclostationary analysis', *Comput Intell Neurosci*, p. 28692.

Hang J. Lee, JAD 2004, *Manual of Nerve Conduction Study and Surface Anatomy for Needle Electromyography*, 4 edn, Lippincott Williams & Wilkins.

Hjorth, B 1975, 'An on-line transformation of EEG scalp potentials into orthogonal source derivations', *Electroencephalogr Clin Neurophysiol*, vol. 39, no. 5, pp. 526-30.

Jasper, HH & Andrews, HL 1938, 'Electro-encephalography. III. Normal differentiation of occipital and precentral regions in man', *Arch Neurol Psychiat*, vol. 39, pp. 95-115.

Kondacs, A & Szabo, M 1999, 'Long-term intra-individual variability of the background EEG in normals', *Clin Neurophysiol*, vol. 110, no. 10, pp. 1708-16.

Kubler, A, Nijboer, F, Mellinger, J, Vaughan, TM, Pawelzik, H, Schalk, G, McFarland, DJ, Birbaumer, N & Wolpaw, JR 2005, 'Patients with ALS can use sensorimotor rhythms to operate a brain-computer interface', *Neurology*, vol. 64, no. 10, pp. 1775-7.

Lal, TN, Schroder, M, Hinterberger, T, Weston, J, Bogdan, M, Birbaumer, N & Scholkopf, B 2004, 'Support vector channel selection in BCI', *IEEE Trans Biomed Eng*, vol. 51, no. 6, pp. 1003-10.

Leeb, R, Friedman, D, Muller-Putz, GR, Scherer, R, Slater, M & Pfurtscheller, G 2007, 'Self-Paced (Asynchronous) BCI Control of a Wheelchair in Virtual Environments: A Case Study with a Tetraplegic', *Comput Intell Neurosci*, p. 79642.

Mason, SG & Birch, GE 2000, 'A brain-controlled switch for asynchronous control applications', *IEEE Trans Biomed Eng*, vol. 47, no. 10, pp. 1297-307.

McFarland, DJ, Sarnacki, WA & Wolpaw, JR 2003, 'Brain-computer interface (BCI) operation: optimizing information transfer rates', *Biol Psychol*, vol. 63, no. 3, pp. 237-51.

Muller-Putz, GR, Scherer, R, Pfurtscheller, G & Rupp, R 2006, 'Brain-computer interfaces for control of neuroprostheses: from synchronous to asynchronous mode of operation', *Biomed Tech (Berl)*, vol. 51, no. 2, pp. 57-63.

Nijboer, F, Sellers, EW, Mellinger, J, Jordan, MA, Matuz, T, Furdea, A, Halder, S, Mochty, U, Krusienski, DJ, Vaughan, TM, Wolpaw, JR, Birbaumer, N & Kubler, A 2008, 'A P300-based brain-computer interface for people with amyotrophic lateral sclerosis', *Clin Neurophysiol*, vol. 119, no. 8, pp. 1909-16.

Noureddin, B, Lawrence, PD & Birch, GE 2008, 'Quantitative evaluation of ocular artifact removal methods based on real and estimated EOG signals', *Conf Proc IEEE Eng Med Biol Soc*, vol. 2008, pp. 5041-4.

Parini, S, Maggi, L, Turconi, AC & Andreoni, G 2009, 'A Robust and Self-Paced BCI System Based on a Four Class SSVEP Paradigm: Algorithms and Protocols for a High-Transfer-Rate Direct Brain Communication', *Comput Intell Neurosci*, p. 864564.

Pfurtscheller, G & Lopes da Silva, FH 1999, 'Event-related EEG/MEG synchronization and desynchronization: basic principles', *Clin Neurophysiol*, vol. 110, no. 11, pp. 1842-57.

Pfurtscheller, G, Muller-Putz, GR, Schlogl, A, Graimann, B, Scherer, R, Leeb, R, Brunner, C, Keinrath, C, Lee, F, Townsend, G, Vidaurre, C & Neuper, C 2006,

'15 years of BCI research at Graz University of Technology: current projects', *IEEE Trans Neural Syst Rehabil Eng*, vol. 14, no. 2, pp. 205-10.

Pfurtscheller, G & Neuper, C 2006, 'Future prospects of ERD/ERS in the context of brain-computer interface (BCI) developments', *Prog Brain Res*, vol. 159, pp. 433-7.

Pfurtscheller, G & Solis-Escalante, T 2009, 'Could the beta rebound in the EEG be suitable to realize a "brain switch"?', *Clin Neurophysiol*, vol. 120, no. 1, pp. 24-9.

Pfurtscheller, J, Rupp, R, Muller, GR, Fabsits, E, Korisek, G, Gerner, HJ & Pfurtscheller, G 2005, '[Functional electrical stimulation instead of surgery? Improvement of grasping function with FES in a patient with C5 tetraplegia]', *Unfallchirurg*, vol. 108, no. 7, pp. 587-90.

Pollock, VE, Schneider, LS & Lyness, SA 1991, 'Reliability of topographic quantitative EEG amplitude in healthy late-middle-aged and elderly subjects', *Electroencephalogr Clin Neurophysiol*, vol. 79, no. 1, pp. 20-6.

Proakis, J & Manolakis, D 2006, 'Digital Signal Processing'.

Raymer, ML, Punch, WF, Goodman, ED, Kuhn, LA & Jain, AK 2000, 'Dimensionality reduction using genetic algorithms', *Evolutionary Computation, IEEE Transactions on*, vol. 4, no. 2, pp. 164-71.

Scherer, R, Lee, F, Schlogl, A, Leeb, R, Bischof, H & Pfurtscheller, G 2008, 'Toward self-paced brain-computer communication: navigation through virtual worlds', *IEEE Trans Biomed Eng*, vol. 55, no. 2 Pt 1, pp. 675-82.

Scherer, R, Muller-Putz, GR & Pfurtscheller, G 2009, 'Flexibility and practicality graz brain-computer interface approach', *Int Rev Neurobiol*, vol. 86, pp. 119-31.

Scherer, R, Schloegl, A, Lee, F, Bischof, H, Jansa, J & Pfurtscheller, G 2007, 'The self-paced graz brain-computer interface: methods and applications', *Comput Intell Neurosci*, p. 79826.

Sellers, EW & Donchin, E 2006, 'A P300-based brain-computer interface: initial tests by ALS patients', *Clin Neurophysiol*, vol. 117, no. 3, pp. 538-48.

Seymour, JP & Kipke, DR 2007, 'Neural probe design for reduced tissue encapsulation in CNS', *Biomaterials*, vol. 28, no. 25, pp. 3594-607.

van Gerven, M, Farquhar, J, Schaefer, R, Vlek, R, Geuze, J, Nijholt, A, Ramsey, N, Haselager, P, Vuurpijl, L, Gielen, S & Desain, P 2009, 'The brain-computer interface cycle', *J Neural Eng*, vol. 6, no. 4, p. 041001.

Verbunt, JA, Seelen, HA, Ramos, FP, Michielsen, BH, Wetzelaer, WL & Moennekens, M 2008, 'Mental practice-based rehabilitation training to improve arm function and daily activity performance in stroke patients: a randomized clinical trial', *BMC Neurol*, vol. 8, p. 7.

Wang, W, Chan, SS, Heldman, DA & Moran, DW 2007, 'Motor cortical representation of position and velocity during reaching', *J Neurophysiol*, vol. 97, no. 6, pp. 4258-70.

Wolpaw, JR, Birbaumer, N, McFarland, DJ, Pfurtscheller, G & Vaughan, TM 2002, 'Brain-computer interfaces for communication and control', *Clin Neurophysiol*, vol. 113, no. 6, pp. 767-91.

Wolpaw, JR & McFarland, DJ 1994, 'Multichannel EEG-based brain-computer communication', *Electroencephalogr Clin Neurophysiol*, vol. 90, no. 6, pp. 444-9.

Wolpaw, JR, McFarland, DJ, Neat, GW & Forneris, CA 1991, 'An EEG-based brain-computer interface for cursor control', *Electroencephalogr Clin Neurophysiol*, vol. 78, no. 3, pp. 252-9.
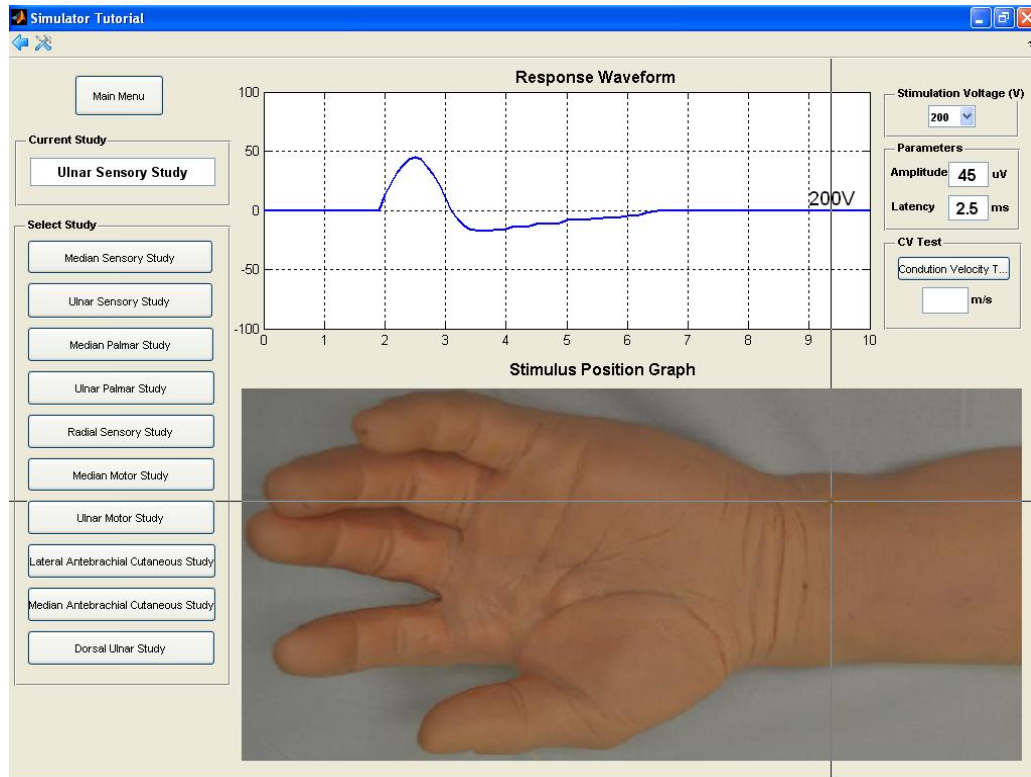
Appendix A.

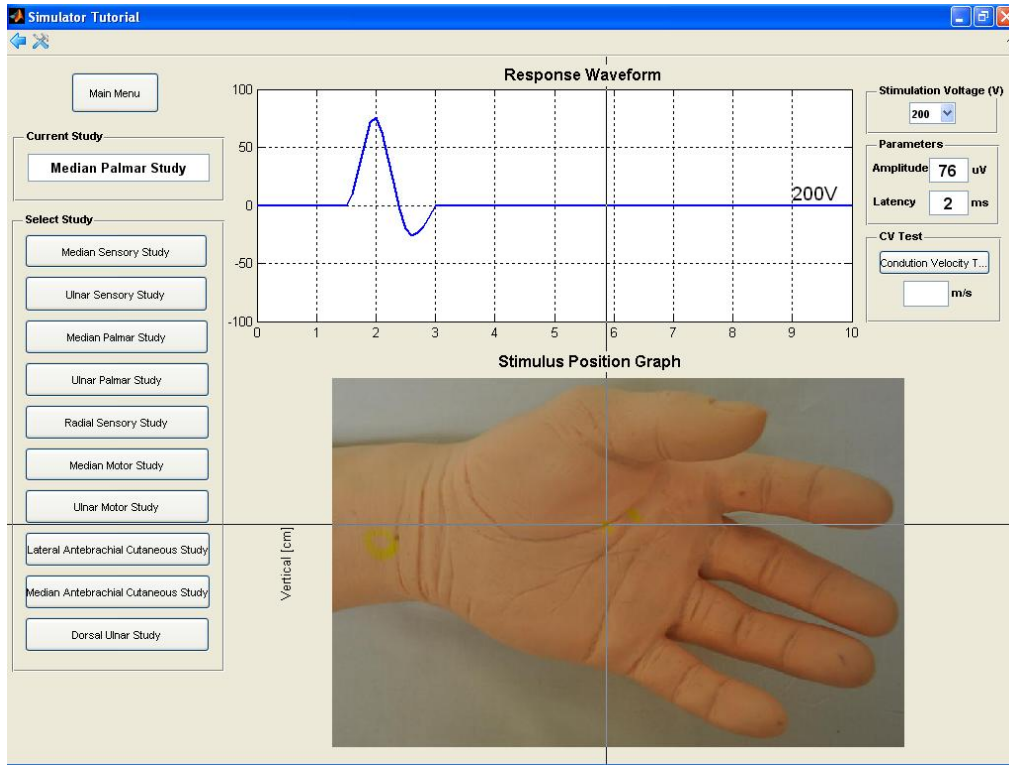## Simulator Interfaces of 10 Studies

1) Median Sensory Study
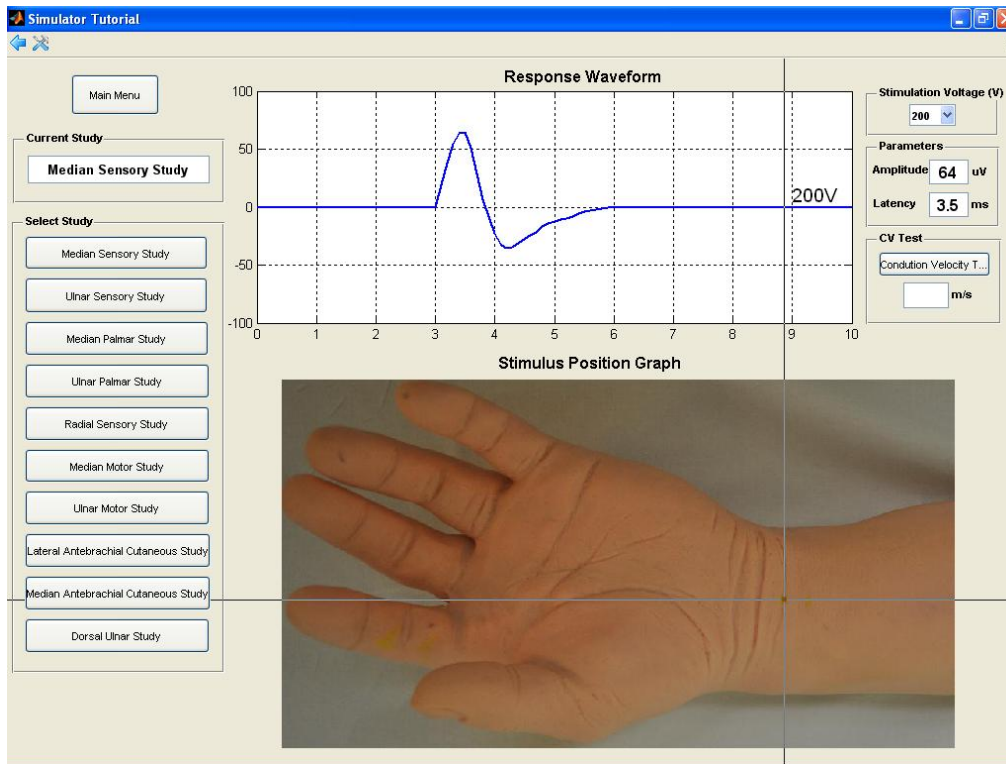
The user can select Median Sensory Study button in select study region on the interface to start study, a crossed mouse cursor will appear as the stimulation stimulator. An arm picture related to the study also appears in the study position region. User can move the cursor around the standard stimulation point, and stimulate with left click. The response waveform of the stimulus will appear in the waveform display region. The parameters of the waveform will display on the right side parameters display region. If the stimulus point is far from the standard stimulation point, a message of out of boundary will display in the wave form region.
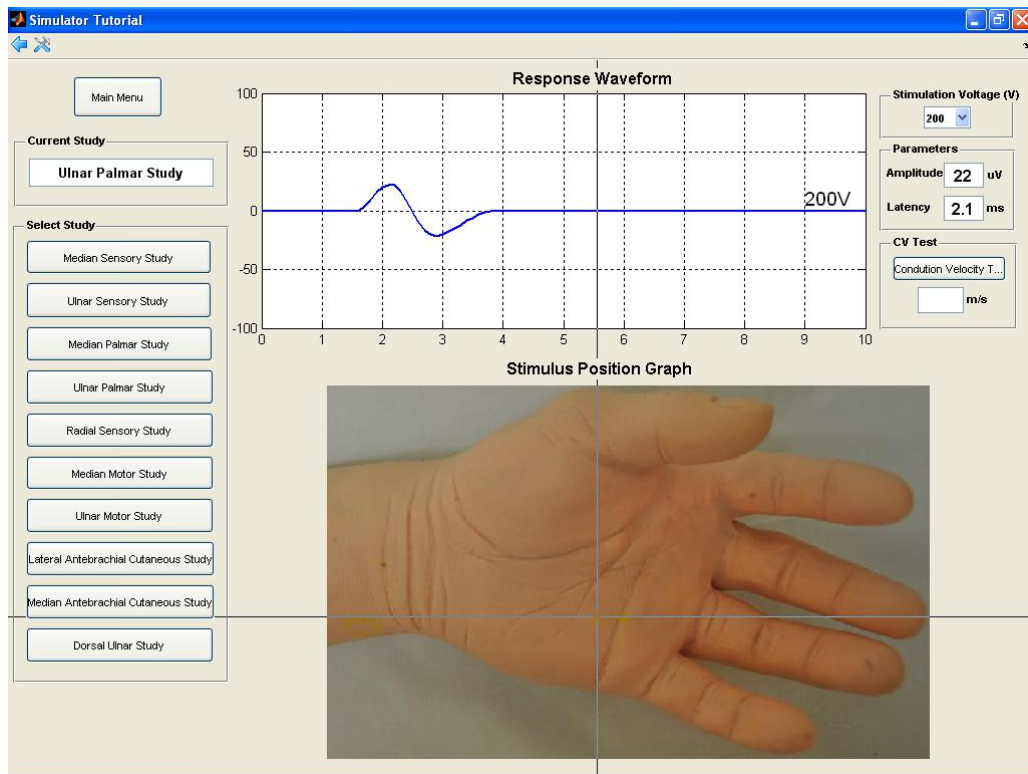
2) Ulnar Sensory Study

The user can select Ulnar Sensory Study button in select study region on the interface to start study, a crossed mouse cursor will appear as the stimulation stimulator. An arm picture related to the study also appears in the study position region. User can move the cursor around the standard stimulation point, and stimulate with left click. The response waveform of the stimulus will appear in the waveform display region. The parameters of the waveform will display on the right side parameters display region. If the stimulus point is far from the standard stimulation point, a message of out of boundary will display in the wave form region.
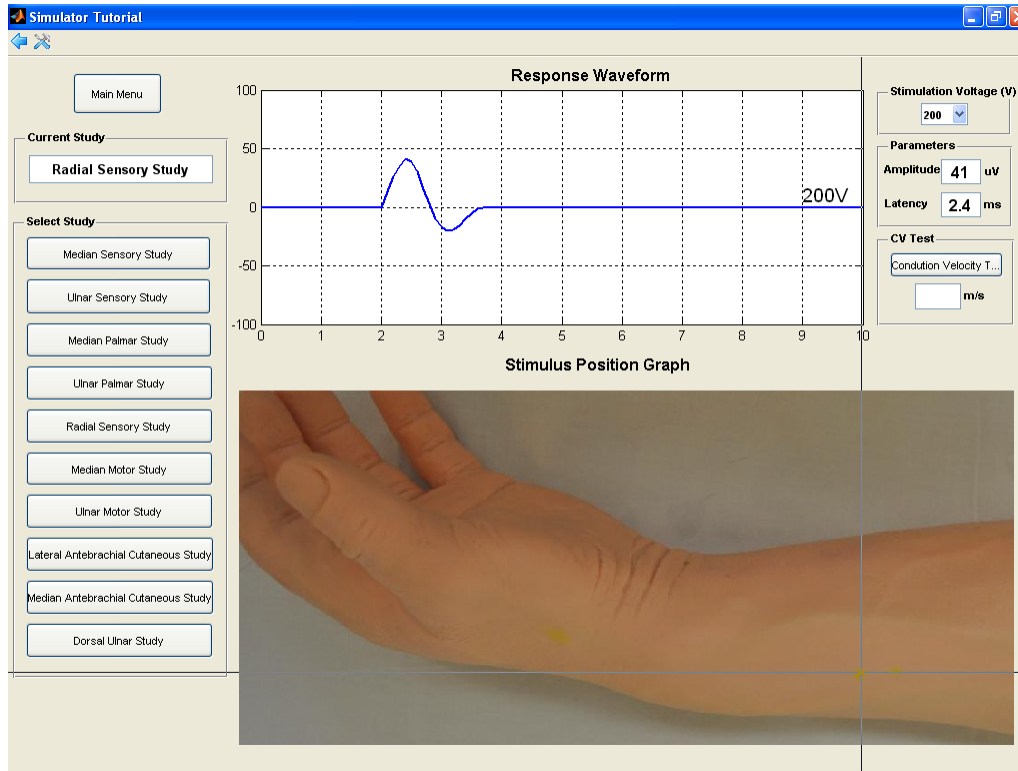
3) Median Palmar Study

The user can select Median Palmar Study button in select study region on the interface to start study, a crossed mouse cursor will appear as the stimulation stimulator. An arm picture related to the study also appears in the study position region. User can move the cursor around the standard stimulation point, and stimulate with left click. The response waveform of the stimulus will appear in the waveform display region. The parameters of the waveform will display on the right side parameters display region. If the stimulus point is far from the standard stimulation point, a message of out of boundary will display in the wave form region.
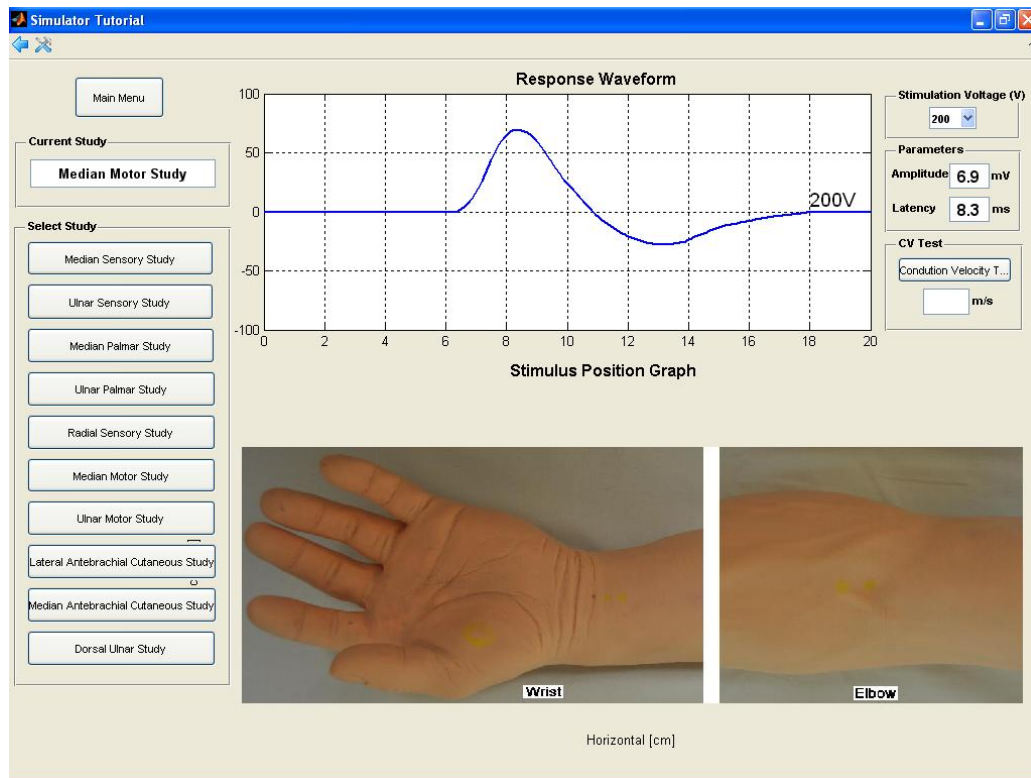
4) Ulnar Palmar Study

The user can select Ulnar Palmar Study button in select study region on the interface to start study, a crossed mouse cursor will appear as the stimulation stimulator. An arm picture related to the study also appears in the study position region. User can move the cursor around the standard stimulation point, and stimulate with left click. The response waveform of the stimulus will appear in the waveform display region. The parameters of the waveform will display on the right side parameters display region. If the stimulus point is far from the standard stimulation point, a message of out of boundary will display in the wave form region.
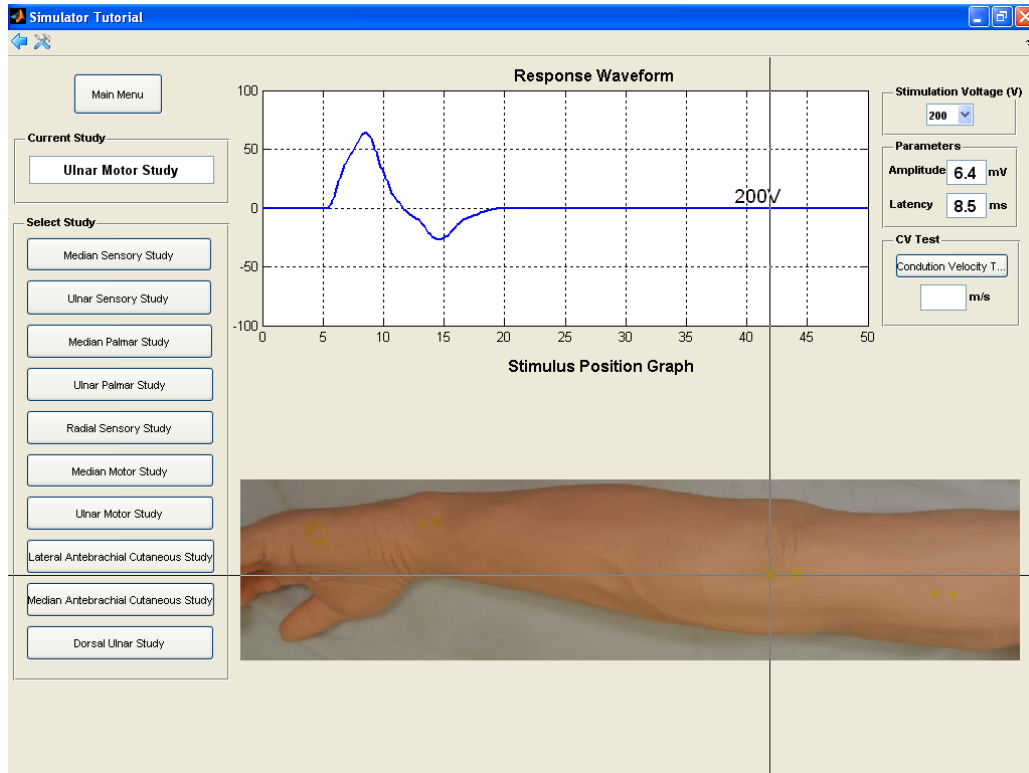
5) Radial Sensory Study

The user can select Radial Sensory Study button in select study region on the interface to start study, a crossed mouse cursor will appear as the stimulation stimulator. An arm picture related to the study also appears in the study position region. User can move the cursor around the standard stimulation point, and stimulate with left click. The response waveform of the stimulus will appear in the waveform display region. The parameters of the waveform will display on the right side parameters display region. If the stimulus point is far from the standard stimulation point, a message of out of boundary will display in the wave form region.
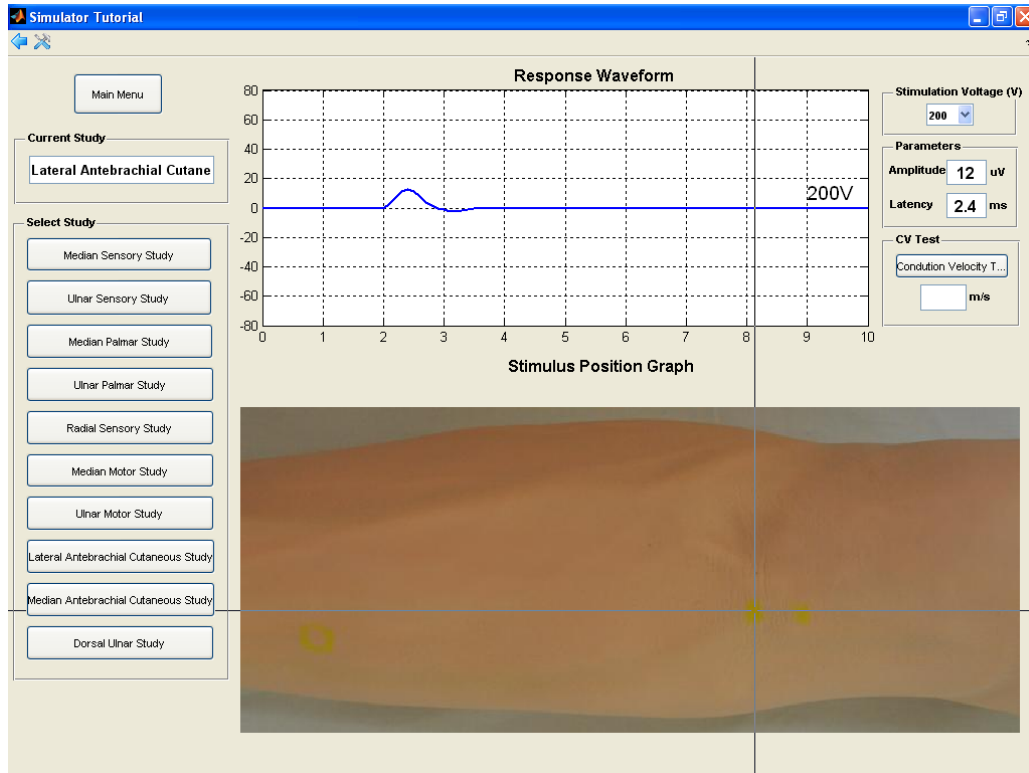
6) Median Motor Study

The user can select Median Motor Study button in select study region on the interface to start study, a crossed mouse cursor will appear as the stimulation stimulator. An arm picture related to the study also appears in the study position region. User can move the cursor around the standard stimulation point, and stimulate with left click. The response waveform of the stimulus will appear in the waveform display region. The parameters of the waveform will display on the right side parameters display region. If the stimulus point is far from the standard stimulation point, a message of out of boundary will display in the wave form region. In motor study, the conduction velocity test is available. Once clicking the conduction velocity test button, the program will wait for two stimulus positions input. User can first stimulate at the distal part and then stimulate at the proximal part of the arm. The conduction velocity value of the segment will display at the parameters display region.
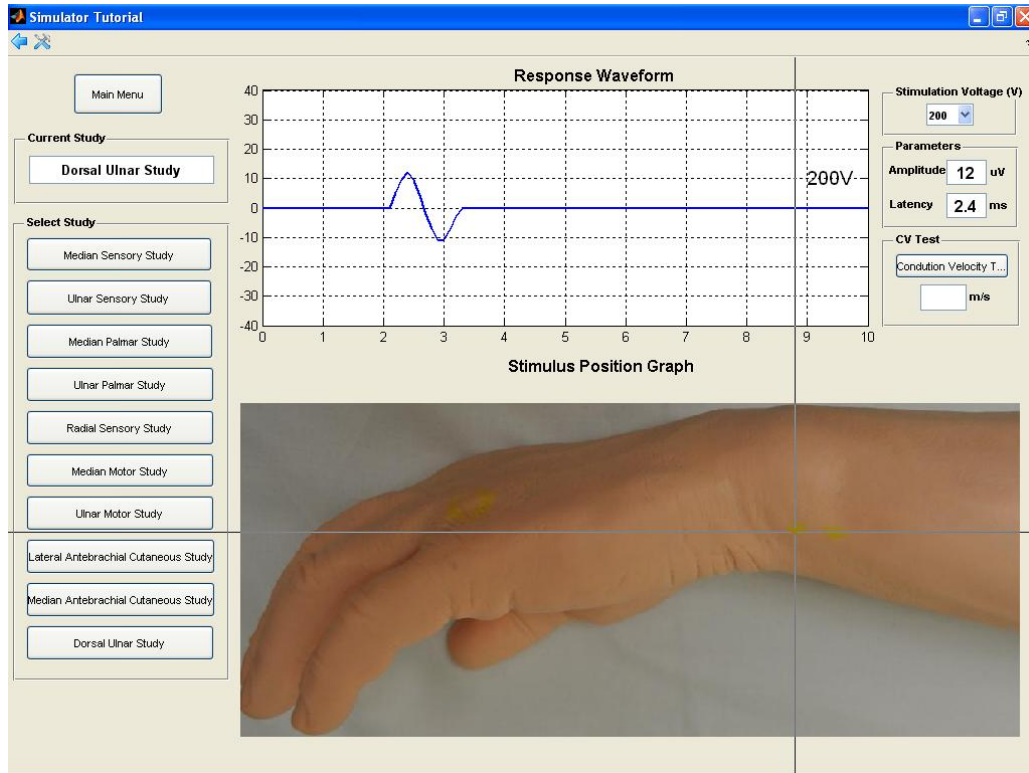
67

7) Ulnar Motor Study

The user can select Ulnar Motor Study button in select study region on the interface to start study, a crossed mouse cursor will appear as the stimulation stimulator. An arm picture related to the study also appears in the study position region. User can move the cursor around the standard stimulation point, and stimulate with left click. The response waveform of the stimulus will appear in the waveform display region. The parameters of the waveform will display on the right side parameters display region. If the stimulus point is far from the standard stimulation point, a message of out of boundary will display in the wave form region. In motor study, the conduction velocity test is available. Once clicking the conduction velocity test button, the program will wait for two stimulus positions input. User can first stimulate at the distal part and then stimulate at the proximal part of the arm. The conduction velocity value of the segment will display at the paramarmeters display region.

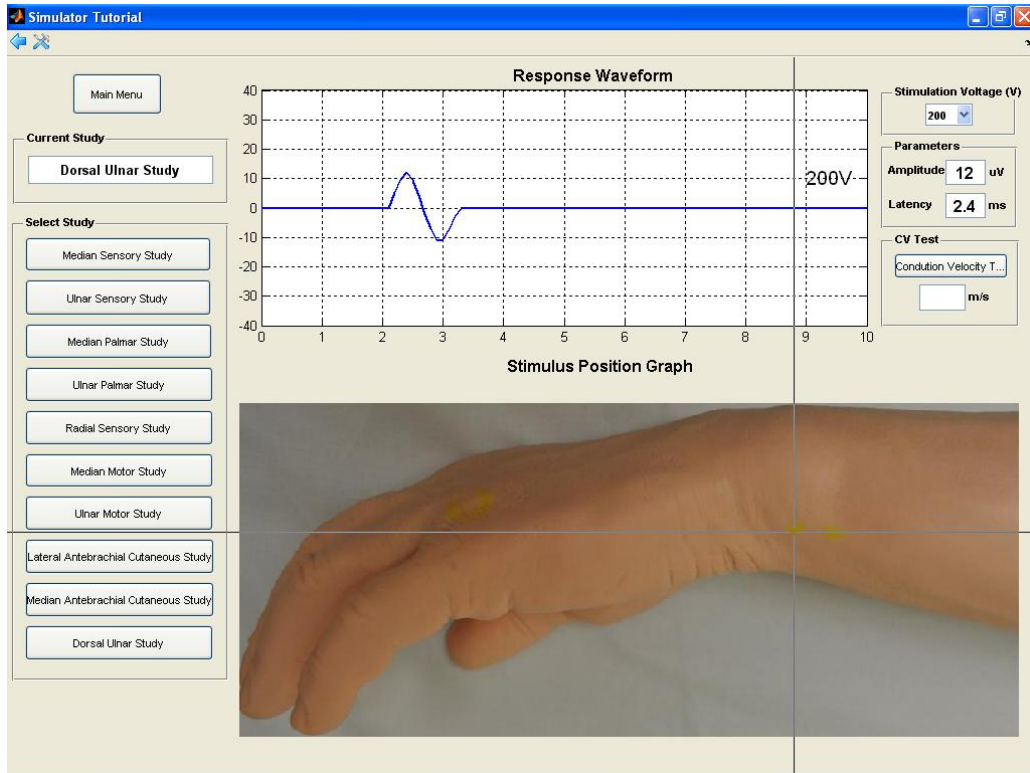## 8) Lateral Antebrachial Cutaneous (LAC) Study

The user can select Lateral Antebrachial Cutaneous Study button in select study region on the interface to start study, a crossed mouse cursor will appear as the stimulation stimulator. An arm picture related to the study also appears in the study position region. User can move the cursor around the standard stimulation point, and stimulate with left click. The response waveform of the stimulus will appear in the waveform display region. The parameters of the waveform will display on the right side parameters display region. If the stimulus point is far from the standard stimulation point, a message of out of boundary will display in the wave form region.

9) Medial Antebrachial Cutaneous (MAC)

The user can select Medial Antebrachial Cutaneous Study button in select study region on the interface to start study, a crossed mouse cursor will appear as the stimulation stimulator. An arm picture related to the study also appears in the study position region. User can move the cursor around the standard stimulation point, and stimulate with left click. The response waveform of the stimulus will appear in the waveform display region. The parameters of the waveform will display on the right side parameters display region. If the stimulus point is far from the standard stimulation point, a message of out of boundary will display in the wave form region.

10) Dorsal Ulnar Study

The user can select Dorsal Ulnar Study button in select study region on the interface to start study, a crossed mouse cursor will appear as the stimulation stimulator. An arm picture related to the study also appears in the study position region. User can move the cursor around the standard stimulation point, and stimulate with left click. The response waveform of the stimulus will appear in the waveform display region. The parameters of the waveform will display on the right side parameters display region. If the stimulus point is far from the standard stimulation point, a message of out of boundary will display in the wave form region.

Vita

Kai Qian was born on Jan 11, 1983 in Malong, Yunnan, China. He got his Bachelor of Engineering degree in 2005 with the major of Automatic Control and minor of Finance at East China University of Science and Technology in China. In Jan 2009, he continued his study in Biomedical Engineering at Virginia Commonwealth University, where he worked as a research assistant. He has been invited to be a member in Phi Kappa Phi Honor Society and is an active graduate member in IEEE Control System Society. His paper entitled "A motor imagery-based online interactive brain-controlled switch: Paradigm development and preliminary test" was published in Clinical Neurophysiology. Currently he is pursuing a Master's degree with the thesis research related with brain-computer interface.

72